MICROCOPY RESOLUTION TEST CHART
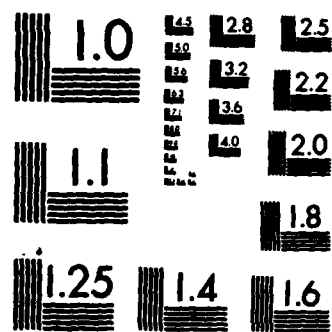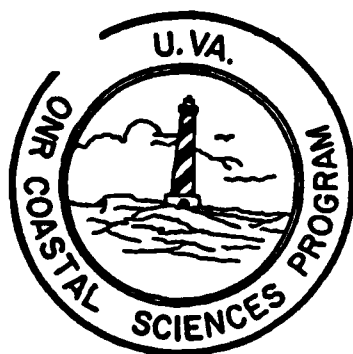
NATIONAL BUREAU OF STANDARDS-1963-A

AD A139947

CLASSIFICATION OF COASTAL ENVIRONMENTS

TECHNICAL REPORT 29

SHOREZONE PROFILE DYNAMICS

ROBERT J. WAYLAND
BRUCE P. HAYDEN

DEPARTMENT OF ENVIRONMENTAL SCIENCES
UNIVERSITY OF VIRGINIA
CHARLOTTESVILLE, VIRGINIA

MARCH 1984

DTIC
ELECTE
APR 0 9 1984
E

84 04 06 012

TABLE OF CONTENTS

Accession For		
NTIS GRA&I	☒	
DTIC TAB	☐	
Unannounced	☐	
Justification		
By		
Distribution/		
Availability Codes		
Dist	Avail and/or Special	
A-1		

DTIC COPY INSPECTED 3

LIST OF FIGURES

iii

LIST OF TABLES

ACKNOWLEDGEMENTS

ABSTRACT

Principal components analysis was used to quantify subaerial and subaqueous summer to winter nearshore morphological change on the North Carolina coast near Duck. The first two eigenvectors explained 61.1% of the total variance. E1 (35.4% of the variance) is a profile rotation and E2 (25.7% of the variance) is a bar/trough function. Two major periods of change were found. High pressure systems in October and extratropical cyclones in November were the weather systems implicated in these changes. These storms caused the profiles to become dissipative. Steepness declined and two bars replaced a single bar profile form. A relationship between pre-existing morphology and subsequent changes in the equilibrium bar/trough morphology was observed during the storm period. Wave characteristics (height, period, steepness, direction, and breaker type) could not be associated with profile changes. The simultaneous offshore sediment movement across three well-defined zones of the shorezone suggests that shore-normal edge waves may be the dominant causative agent for these changes.

INTRODUCTION

Along most of the U.S. coast north of South Carolina there are either one or two shore-parallel bars. Based on the analysis of color infrared aerial imagery along the mid-Atlantic coast between 1970-1979, Kochel et al. (1983) determined that there is little temporal stability in the number of bars present from Cape Lookout north. Aerial photography taken over the last decade near the the Army Corps of Engineers, Field Research Facility, Duck, North Carolina, showed double bars normally occurring during winter, while only a single bar was normally present during summer months (Table 1) (Kochel et al. 1983, 1984). The only previous mention of a seasonal transition in the number of bars present along a coast comes from Shepard (1950). He observed the presence of a single bar along a portion of the California coast in winter and the absence of a bar in summer. Conventional wisdom (Evans, 1940) and theoretical studies (Lau and Travis, 1973; Carter, Liu and Mei, 1973) indicate that the number of bars present is a function of the overall slope of the nearshore bottom - the more gradual the slope, the greater number of bars.

Empirical studies using multivariate statistical analyses of inshore profiles clearly indicate a statistical independence between the slope of the profile, the curvilinear form of the profile, and the number of bars in the profile (Hayden et al., 1975, Resio et al., 1974, Dolan et

-1-

WINTER		SUMMER	
Date	# of Bars	Date	# of Bars
1-30-73	2	6-04-74	1
2-25-75	1	9-05-75	0
2-02-77	1	7-29-77	1
3-02-77	2	9-13-78	1
2-02-78	2	4-11-79	1
10-18-78	1	4-12-79	1
12-02-78	1	9-20-79	2
10-15-79	1	4-04-80	1
1-16-80	2	7-15-80	1
3-24-81	2	8-27-81	1
2-02-81	1	9-24-81	1
10-27-82	2	5-11-82	1
		7-04-82	1

TABLE 1 : Bar patterns approximately 500 meters north and south of the CERC pier as evidenced by breaker lines in 25 individual sets of aerial photography. Winter season corresponds to October - March, while Summer refers to April - September. (Kochel et al., 1984)

al., 1982). It is unlikely that slope variations at a site are responsible for the temporal instability of bar numbers along the east coast. Our understanding of the nature and causes of changes in nearshore bathymetry is based largely on laboratory and theoretical studies. Spatially and temporally extensive, systematic, and ongoing beach observational programs have only recently begun at Duck, North Carolina.

The summer to winter morphological transition in the subaerial and subaqueous nearshore zone at Duck, North Carolina is studied in this report. Specifically, we examine the role of various synoptic weather systems as agents of change in the sedimentary prism; the importance of wave height, period, direction, steepness and breaker type relative to profile changes; and the role played by existing profile form on this seasonal change in nearshore morphology.

LITERATURE REVIEW

The literature on causes of changes in beach profiles can be divided into contributions that focus on the role of pre-existing morphology, storms, incident waves, and edge waves. The concept that morphological changes are a function of the pre-existing morphology implies an ordered sequence of change. Sonu and Van Beek (1971) offered such a model of sequential beach changes based on data collected

along the Outer Banks of North Carolina (Dolan, 1966), and they proposed a linkage between rhythmic topography and shore-normal profile change. Their along-the-coast study reach was limited to tens of meters, however. The model they developed allowed the prediction of successive beach profiles based on pre-existing sediment storage, beach width and surface configuration.

More recently Wright et al. (1979) proposed a model of sequential beach changes relating to surf zone morphodynamics based on studies of Australian beaches. Two major types of beaches were identified: steep, reflective beaches and flat, dissipative beaches. Steep, reflective beaches have well-developed berms and beach cusps, and surging breakers with high runup and minimum setup. Rip currents and the associated three dimensional inshore topography are absent in steep, reflective beaches. Flat, dissipative beaches have wide surf zones, much more complex nearshore topography (than reflective systems), and rip cells. Short (1979), also working on Australian beaches, observed sequential bar stage development which he described in a three-dimensional model of ten stages. These changes in the observed beach morphology were related to the cumulative wave power.

Storm waves have been recognized as modifying agents on beaches for many years (Zeigler, et al., 1959; Fox and Davis, 1976; Dolan and Hayden, 19'1). Zeigler et al. (1959)

found that storms along Outer Cape Cod, Massachusetts, caused rapid changes in beach volume and topography. Their study concluded that after storms, profiles were either planar or concave upward, while during quiescent periods they were convex upward. In a more recent study, Fox and Davis (1976) investigated the responses of coastal systems to atmospheric (storm) processes. Working with data from the eastern shore of Lake Michigan; Mustang Island, Texas; and the central Oregon coast, they developed a coastal process-response model. Time series analyses of weather, waves and current data were combined with frequent beach profile data to construct the model. The study concluded that morphologic responses differed in the three areas because their positions relative to storm tracks, coastal orientation, tidal range, and nearshore topography were different. Dolan and Hayden (1981) examined the along-the-coast periodicities in storm overwash following the Ash Wednesday Storm of March 1962. This study concluded that the location and magnitude of storm deposits and storm hazards were systematically distributed along the Atlantic Coast.

Goldsmith et al. (1982) delineated sequential bar development patterns at Hahoterim Beach, Israel. These changes were found to be induced by changes in the incident wave energy of the area, and the threshold values for these morphologic transitions were quantified. They concluded

that double-crescentic patterns were the optimal evolutionary stage of crescentic systems, and that outer bars and mega-rip channels composed the most stable inshore elements. Aubrey et al. (1980) developed a linear statistical estimation model (based on empirical eigenfunctions) to predict changes in beach profiles, using variations in incident wave energy. They concluded that weekly mean wave energy was the best predictor of beach changes.

Rhythmic coastal topography has been explained in several ways: intersecting wave trains, variations in nearshore topography, and edge waves. The concept of edge waves as morphologic agents has been investigated by many researchers (Dalrymple, 1975; Bowen and Inman, 1971; Guza and Inman, 1975; Dolan et al., 1979). Edge waves are normal trapped modes of longshore periodic wave motions. These motions occur along the edge of water bodies and may be one of two distinct types: standing or progressive. These phenomena can be found on straight or curving shorelines, as well as on concave or convex offshore slopes. Their inability to radiate energy into deeper water causes them to dissipate their energy only through friction and interaction with other currents and wave forms (Guza and Inman, 1975).

Guza and Inman (1975) analyzed beach cusps in reflective systems from both analytical and observational approaches. They found that the edge wave resonances, theoretically predicted and observed, were not visible on the beach face during plunging incident wave conditions.

In a more recent study, Dolan et al. (1979) used the edge wave phenomenon to explain the longshore periodicities along the Cape Hatteras Arc. They noted that standing edge waves, unlike intersecting wave trains and inshore topography, would result in both temporal and spatial stability of the shore face features. They concluded that edge waves were important in determining the intensity of regional-scale morphodynamic responses along the mid-Atlantic coast barrier islands.

STUDY SITE

The Coastal Engineering Research Center (CERC) has been conducting coastal research for over twenty years. Field observations supportive of earlier experimental and theoretical investigations lacked accurate, repetitive wave, beach and water level data, however, especially during storms. To meet the need for such data the Field Research Facility (FRF) was constructed near Duck, North Carolina (Fig. 1). Located at $36^{o}10'$ north latitude and $75^{o}45'$ west longitude, the FRF's 561 m research pier and the 418 m^2 laboratory and office building were completed in 1976 and 1980, respectively (Birkemeier, et al., 1981). The addition of the Coastal Research Amphibious Buggy (CRAB) to the FRF's data collection facilities in 1981 has improved the quality, density and resolution of CERC's profile data base.

The coast at the FRF is part of an unbroken 100 km stretch of coastline extending south from Rudee Inlet,
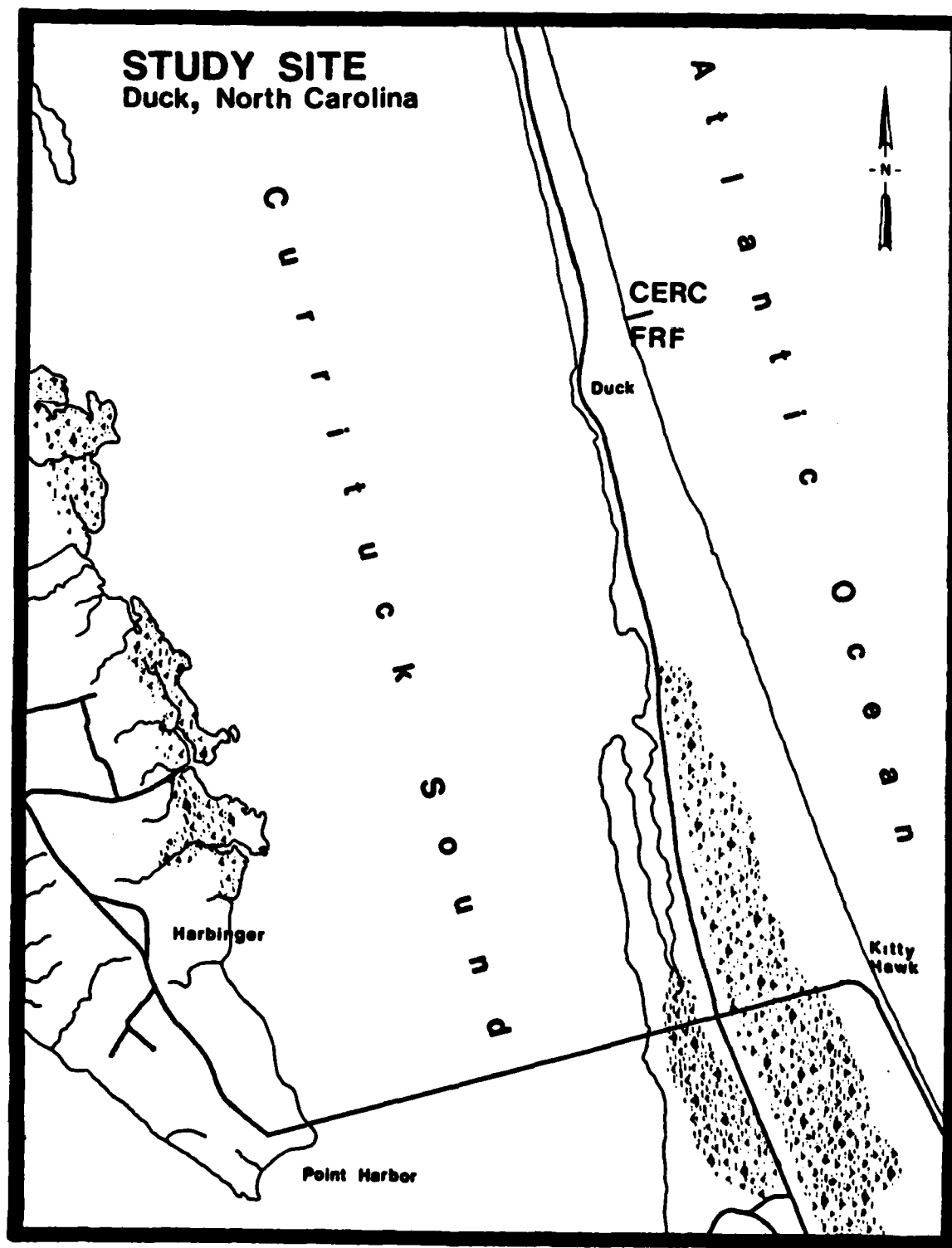
FIGURE 1 : Location of the coast near the Coastal Engineering
            Research Center, Field Research Facility, Duck, North
            Carolina.

Virginia, to Oregon Inlet, North Carolina. This long, narrow barrier island is part of the Outer Banks, North Carolina. The area is subject to winds and waves from intense high pressure cells as well as tropical and extra-tropical low pressure cells. The climate is temperate marine with mild winters and warm summers (Birkemeier et al., 1981).

Forewarning of storms is difficult in this area because cyclogenesis often occurs offshore from Cape Hatteras, North Carolina. Bosserman and Dolan (1968) determined that the most damaging storms follow northeast tracks off the mid-Atlantic coast. The highest winds and waves tend to occur when low pressure storm movement is blocked by a high pressure system to the north. Hayden (1981) calculated the mean extratropical cyclone frequency for Eastern North America in 2.5° latitude by 5.0° longitude grid cells. His results showed a storm frequency maximum along the east coast baroclinic zone. Tropical cyclone frequencies along the North Carolina coast are variable. The area between Cape Lookout and Cape Hatteras has the highest frequency of hurricane occurrence, while the area around the FRF has the lowest.

STORM-WAVE EVENTS

During the nine-month survey period, six synoptic scale weather events occurred that caused winds of sufficient magnitude to generate wave heights in excess of 2 m at

the Field Research Facility. These events were divided into three major categories: tropical storms/hurricanes, extra-tropical storms, and high pressure systems. There were two examples of each storm type during the study period. The significant environmental variables for each of the events are summarized in Table 2.

Hurricane Dennis, the first 1981 tropical storm to effect the study area, originated from an African distur-bance and was named on August 8, 1981, while centered 800 km southwest of the Cape Verde Islands. The system tracked westward across the Atlantic and Caribbean, nearly stalling on August 14 south of Cuba. On August 15, Dennis reinten-sified and turned northward across Cuba and toward the southeastern United States. Dennis travelled parallel to the east coast before turning northeastward away from the middle Atlantic states on August 20. The highest sustained surface wind reported by a land station was 20 m/s at Cedar Island, North Carolina. Dennis reached hurricane status for approximately 12 hours on August 20, after which the storm center moved over colder waters and lost its tropical characteristics by August 22. Maximum sustained winds were 36 m/s and the lowest central pressure was 995 mb (Lawrence and Pelissier, 1982)

Hurricane Emily formed on a frontal wave in a manner similar to Cindy (August 2-5, 1981). The storm tracked northeastward toward Bermuda. The storm system's forward

SURVEY NUMBER	SURVEY DATE	STORM EVENT	DURATION	OBSERVED BREAKER TYPES			MAX WAVE HEIGHT	MAX WAVE STEEP	MAX WAVE LENGTH	MAX WAVE PERIOD	MEAN WAVE ANGLE	MEAN WIND SPEED	MEAN WIND DIR.	MAX WATER ELEV.	MAX TIDAL RANGE	*
				PLG	SPL	SRG										
3	8-4-81															
		Hurricane Dennis 8/18-8/23	6 DAYS	X	X		2.94m	0.034	261.1m	12.9m/s	58°	18m/s	97°	1.44m	1.44m	+
4	8-24-81															
		Hurricane Emily 9/3-9/8	6 DAYS	X	X		2.58m	0.010	270.3m	13.2m/s	79°	8m/s	206°	1.02m	1.13m	-
5	9-19-81															
		High Pressure 1 10/11-10/17	7 DAYS	X	X		2.50m	0.035	230.7m	12.2m/s	64°	15m/s	69°	1.25m	1.51m	+
		High Pressure 2 10/28-11/2	6 DAYS	X	X		2.25m	0.029	232.0m	12.2m/s	72°	13m/s	80°	1.01m	1.24m	+
6	11-3-81															
		Low Pressure 1 11/11-11/17	7 DAYS	X	X	X	3.26m	0.271	279.1m	13.3m/s	52°	18m/s	197°	1.58m	1.78m	+
7	11-16-81															
		Low Pressure 2 11/24-11/27	4 DAYS	No Data Avail.			2.48m	0.216	329.9m	14.5m/s	61°	8m/s	260°	1.13m	1.21m	+
8	1-5-82															

*Dominant Longshore Current Direction(+)--indicates southerly flowing current; (-)--indicates northerly flowing current

TABLE 2 : Summary of significant environmental variables for the six storm events, at the CERC, FRF.

progress was temporarily impeded by a high pressure system passing to the north, causing the tropical storm to make a small, counterclockwise loop on September 3, 1981. It was during this loop phase that Emily tracked westward and posed its greatest threat to the middle Atlantic region. On September 4, Emily began to move northeastward and back out to sea. Maximum surface winds of 41 m/s (and a minimum surface pressure of 966 mb) were reached on September 6, (Lawrence and Pelissier, 1982).

On October 11, 1981, the first of two consecutive strong high pressure systems formed in the Maritime Provinces of Canada. This high intensified and moved into the New England States on the 13th. A strong pressure gradient and onshore winds prevailed at the FRF throughout the duration of the event. By the 15th, the ridge had weakened and the gradient deteriorated as the high moved off the coast of Maine. The maximum pressure reading (1036 mb) was observed on October 13, at 1200 GMT.

A second, stronger high pressure cell formed in the same region as the first on October 29, 1981. This system also produced strong pressure gradients normal to the east coast, with persistent onshore winds. The maximum pressure (1042 mb) was observed on October 31, while the high was centered over northern Maine. The system dissipated as it tracked eastward off the New England coast.

The first extratropical storm event of the season formed over the southwestern United States. The storm

travelled southeastward into the Gulf of Mexico and traversed Florida on November 11, 1981. By November 13, the storm was centered off Cape Hatteras and ships in this area were reporting 40-50 knot winds with waves in excess of 30 feet. At 7:00 A.M. EST on the 15th, the storm was centered at approximately 38°N latitude and 72°W longitude and had a central pressure of 984 mb. The combination of the low pressure cell and a syzygy-perigean alignment of the sun, moon and earth resulted in high waves and water levels at the study site (Miller and Leffler, 1981). The storm continued to track northeastward, crossing Newfoundland by the 18th (Mariner's Weather Log, 1982).

On November 24, 1981, a secondary low was triggered off the South Carolina coast as a low pressure cell moved into the Appalachian Mountains of the Carolinas. By 7:00 A.M. on the 25th, the storm had depressed to 980 mb and was located off Cape Hatteras. An offshore buoy recorded 26 foot wave heights, and winds at Cape Hatteras exceeded 50 knots. By November 26, the storm was 972 mb, but it was located well out to sea (40°N, 57°W) (Mariner's Weather Log, 1982).

DATA SET

Profile data were collected at the Field Research Facility (FRF), Duck, North Carolina, by the U.S. Army Corps of Engineers, using the Coastal Research Amphibious Buggy

(CRAB). The CRAB is a 10.7 m high amphibious tripod vehicle capable of operating in water depths up to 9 m and wave heights up to 1.8 m. Position and profile elevation are determined using the CRAB-Zeiss surveying system; a Zeiss Elta-2 first order, self-recording electronic distance meter in combination with the CRAB (Birkemeier et al., 1981 and Miller and Leffler, 1982).

Ten bathymetric surveys containing 11 individual profile lines were evaluated in this study (Fig. 2). The study period spanned nine months between July 2, 1981, and March 18, 1982 (Table 3). Environmental variables for the corresponding storm periods were also collected at the FRF, and reported in the monthly Basic Environmental Data Summary, published by CERC. Daily values for barometric pressure, wind speed, wind direction, wave height, wave period, and longshore current direction were used in this study.

The profile data were organized for analysis in two ways: shore parallel transects and shore normal transects (traditional method). The profile lines normal to the shore each contain 44 elevation points (variables) beginning 60 m seaward of the FRF baseline and extending to 760 m from the baseline. This entire data matrix is 44 variables by 110 cases. The shore parallel data are structured as an 11 variable by 440 case data matrix. The shore-parallel data matrix is further subdivided into two groups; one for profiles north of the pier and the other for profiles south
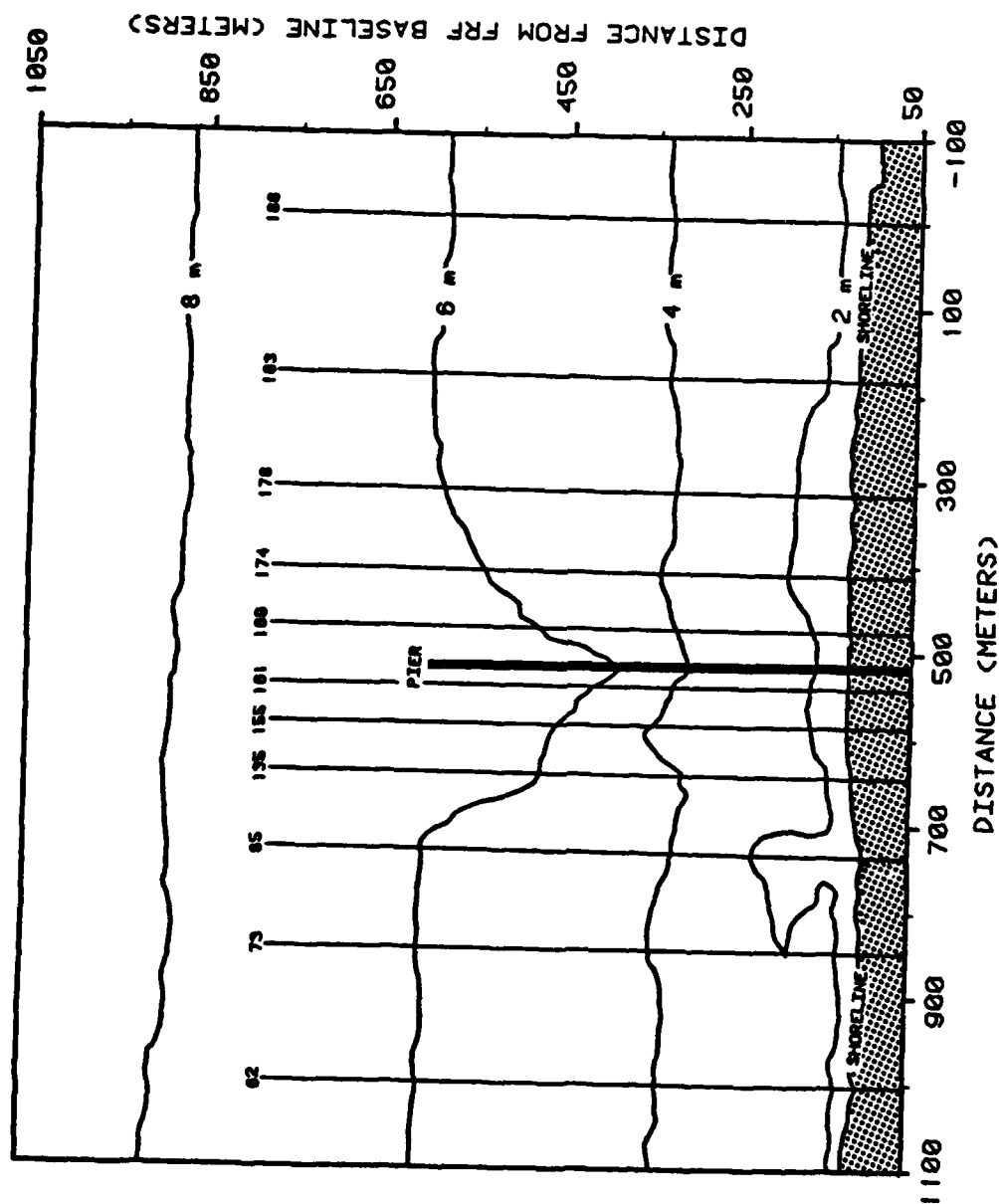
FIGURE 2 : Location of Coastal Research Amphibious Buggy profile lines at the FRF. Contours indicate water depths in meters. In this study, CERC profile line 62 will be referred to as profile line 1, CERC profile line 73 as line 2.....CERC profile line 188 as line 11.

Survey 1: July 2, 1981

Survey 2: July 17, 1981

Survey 3: August 4, 1981

Survey 4: August 24, 1981

Survey 5: September 19, 1981

Survey 6: November 3, 1981

Survey 7: November 16, 1981

Survey 8: January 5, 1982

Survey 9: February 9, 1982

Survey 10: March 18, 1982

TABLE 3: Bathymetric survey dates during the study period at the FRF.

of the pier. These profile data sub-sets contain 220 cases
each and six and five variables, respectively.

THE ANALYSIS

Principal components analysis was used to define the
modes of intercorrelation that exist among the variables
(profile elevation points). The analysis was designed to
delineate both the shore-parallel and the shore-normal
variations in nearshore morphology.

Principal components analysis has been successfully
used to partition the variance in multivariate geophysical
data sets (Kutzbach, 1967; Resio et al., 1974; Hayden et
al., 1975; Aubrey, 1979; Aubrey et al., 1980; Hayden, 1981;
Dolan et al., 1982). Using a minimization of least square
errors, this method of analysis is useful for determining
patterns in large data sets (Lorenz, 1956; Gilman, 1957;
Kutzbach, 1967). Principal components analysis transforms a
series of intercorrelated variables into a set of new
statistically independent variables. These new variables
are linear combinations of the original variables but are
mutually orthogonal. Principal components analysis was
chosen in this study because profile elevation variations
are quantified and organized in the first few principal
components, and because the principal component eigenvectors
and their weightings in time can be related directly to the
physical environment.

RESULTS

Means and Standard Deviations

Fig. 3 shows the mean profile elevations along with standard deviations of these elevations at each of the 44 intervals along the profile line. A single bar is located approximately 340 m from the baseline (station number 27). The remainder of the profile is featureless. Maximum standard deviations occur in the center of the profile (points 17-21), and decrease both landward and seaward. As noted in the Horn Island, Mississippi data collected by Dolan et al. (1982), there is no variance maxima in the vicinity of the bar (point 27). The means and standard deviations of the profile elevation points are given in Table 4.

Fig. 4 shows the means of the 11 profiles at each survey date. At the time of the July 2, 1981, survey, a single inshore bar was centered 220 m from the baseline. The July 17, 1981, and August 4, 1981, mean profiles showed a slight filling of the inner trough. Hurricane Dennis' passage caused a seaward displacement of the bar out to 280 m from the baseline in the August 24, 1981, survey. The trough also deepened slightly during this time.

By the September 19, 1981, survey, a double-bar profile had evolved with a broad inner bar centered 100 m from the baseline and a small outer bar located approximately 300 m from the baseline. There was a substantial
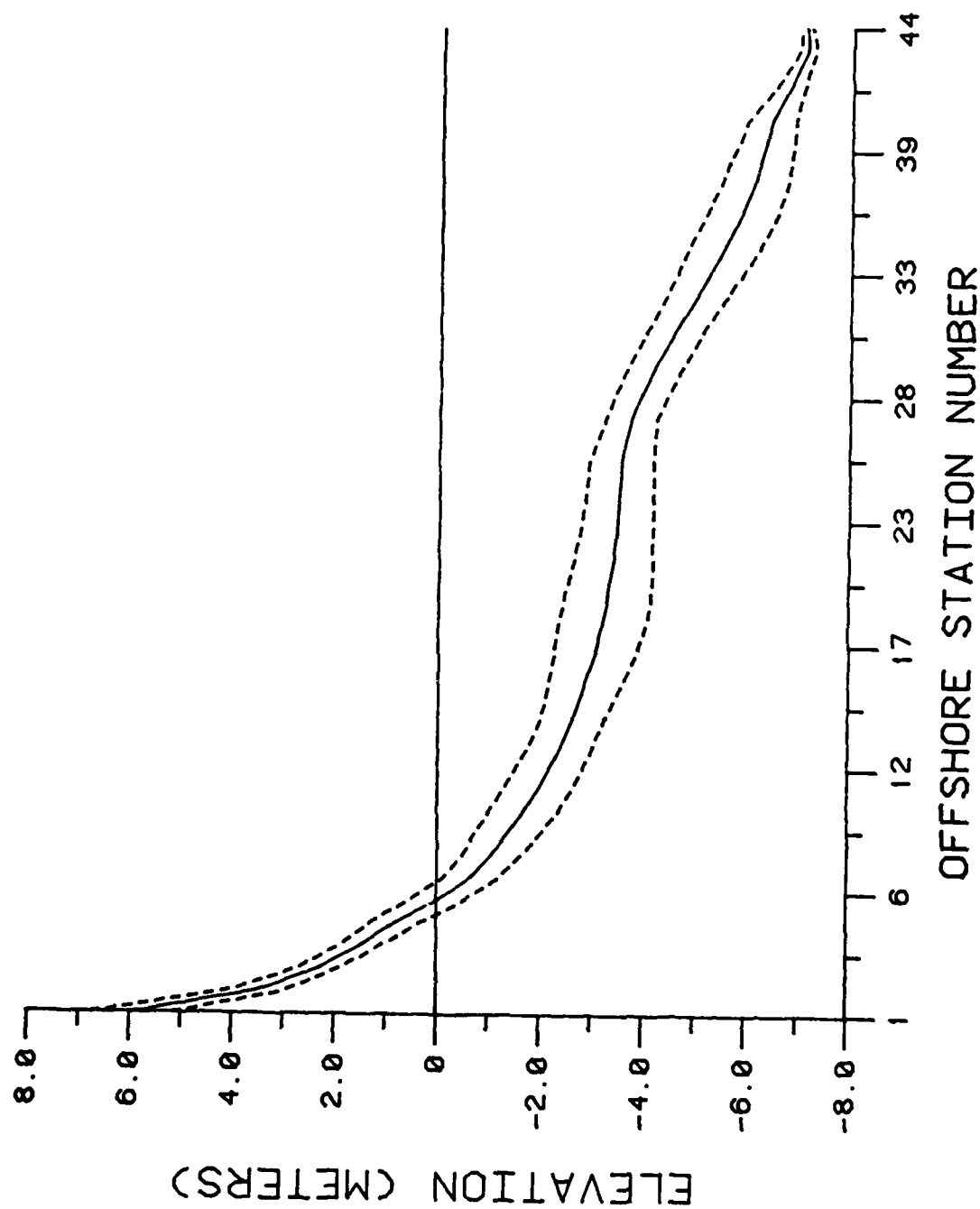
FIGURE 3 : The mean profile plus-or-minus one standard deviation at the FRF.

OFFSHORE STATION NUMBER	DISTANCE FROM BASELINE*	DISTANCE OFFSHORE*	MEAN*	STANDARD DEVIATION
1	60	---	5.9	.8
2	70	---	3.5	.6
3	80	---	2.3	.4
4	90	---	1.5	.4
5	100	---	0.8	.5
6	110	0	0.0	.5
7	120	10	-0.7	.5
8	130	20	-1.1	.6
9	140	30	-1.4	.6
10	150	40	-1.7	.7
11	160	50	-2.0	.7
12	170	60	-2.2	.7
13	180	70	-2.5	.6
14	190	80	-2.7	.6
15	200	90	-2.8	.7
16	210	100	-3.0	.8
17	220	110	-3.1	.8
18	230	120	-3.2	.9
19	240	130	-3.3	.9
20	250	140	-3.4	.8
21	260	150	-3.4	.8
22	270	160	-3.5	.7
23	280	170	-3.5	.7
24	290	180	-3.5	.7
25	300	190	-3.6	.6
26	320	210	-3.6	.6
27	340	230	-3.8	.5
28	360	250	-3.9	.5
29	380	270	-4.1	.5
30	400	290	-4.4	.5
31	420	310	-4.6	.6
32	440	330	-4.9	.6
33	460	350	-5.2	.6
34	480	370	-5.4	.7
35	500	390	-5.7	.7
36	520	410	-5.9	.7
37	540	430	-6.1	.7
38	560	450	-6.2	.6
39	580	470	-6.3	.5
40	600	490	-6.4	.5
41	640	530	-6.7	.3
42	680	570	-6.9	.2
43	720	610	-7.1	.2
44	760	650	-7.1	.1

* These values are expressed in meters (m).

TABLE 4 : The mean elevation (measured from MSL) and standard deviation for each of the 44 stations along shore-normal profiles. Station locations are measured from both the CERC baseline and the shoreline.
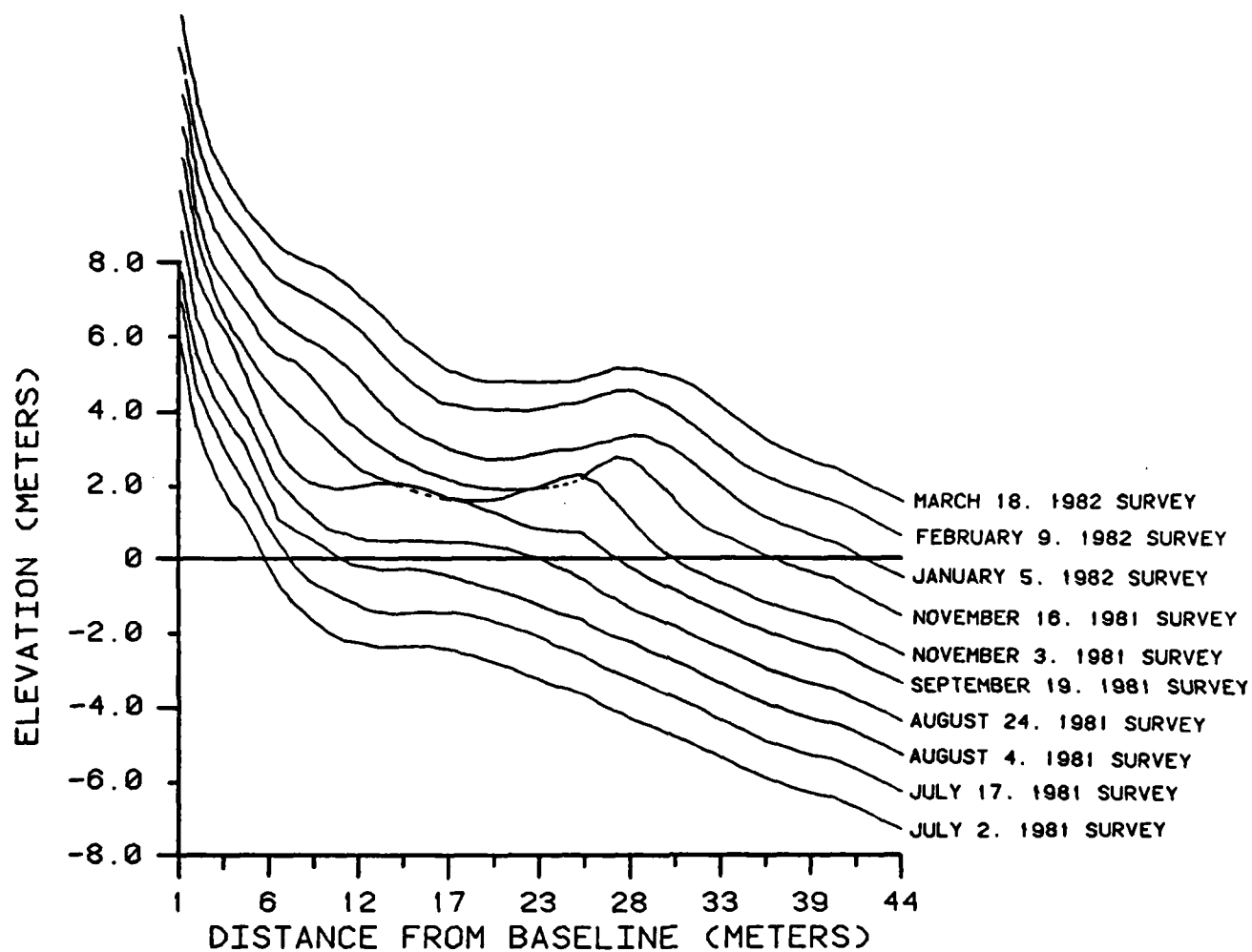
FIGURE 4 : The mean FRF profiles for each survey date. The profiles are offset by 1 (one) meter intervals.

amount of erosion in the berm area following this survey. The November 3, 1981, mean profile had a well developed storm bar 300 m from the baseline, with a broad inner trough. Berm destruction continued through this survey period. Maximum development of the storm bar occurred by the November 16, 1981, survey. The outer bar had moved 60 m farther offshore and a small inner bar had developed 140 m from the baseline.

The survey of January 5, 1982, showed an increase in size of the inner and outer bar systems, and both bars were slightly farther offshore relative to the previous survey. The February 9, 1982, mean profile showed no change seaward of the outer bar, while sediment deposition occurred landward of this point. The final survey, March 18, 1982, showed a slight broadening of the outer bar with little or no change in the nearshore areas.

The Eigenvectors

The percent of variance explained in each of the first four eigenvectors of the correlation matrix is summarized in Table 5 for shore normal profile data. The Monte Carlo test of Overland and Preisendorfer (1982) for statistical significance of the eigenvectors was used here. The first four eigenvectors explained 84.4% of the total variance. Each of these vectors explained a greater percentage of the variance than are explained by 95% of the same order vectors computed from random data matrices of the same dimensions. Geophys-

EIGENVECTOR	PROFILE DATA Variance Explained		RANDOM DATA (.05 Significance Level)
	Individual	Cumulative	(Overland & Preisendorfer, 1982)
E1	35.35%	35.35%	6.94%
E2	25.73%	61.08%	6.47%
E3	13.12%	74.20%	5.92%
E4	10.18%	84.38%	5.56%

TABLE 5 : Percent of the total system variance explained by the profile data and random data.

ical significance was determined by inspection and study of each individual eigenvector and its variation in space and time.

The first four eigenvectors, those that are statistically significant at the .05 level, were examined (Fig. 5a, 6a, 7a, and 8a). To aid in the interpretation of the eigenvectors, profile elevations were reconstructed by adding the variation explained by each eigenvector according to

$$\bar{R}_{ij} = \bar{X}_i \pm C \ (SD_i) \ (E_{ij})$$

where $\bar{R}_{ij}$ is the reconstructed value for the ith point along the profile of the jth eigenvector. $\bar{X}_i$ is the mean profile elevation at the ith point along the profile. SD_i is the standard deviation of profile elevation at the ith point along the profile. and E_{ij} is the weighting on the jth eigenvector for the ith point along the profile. $\pm C$ is a constant which is representative of the case weightings (time series) on a particular vector. Plots of R_{ij} at each profile point for representative positive and negative C values (Table 6) are shown in Fig. 5b, 6b, 7b, and 8b.

The average case loading (Δ_t) for the jth eigenvector at k^{th} profile location over all survey dates is given by

$$\Delta t = \frac{1}{10} \sum_{t=1}^{10} E_{ijk}$$

at each k and for j=1 to 4. These case loadings are shown in Fig. 5c, 6c, 7c, 8c.
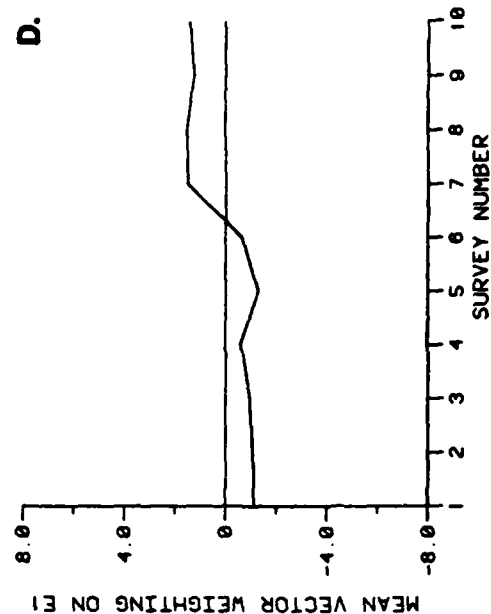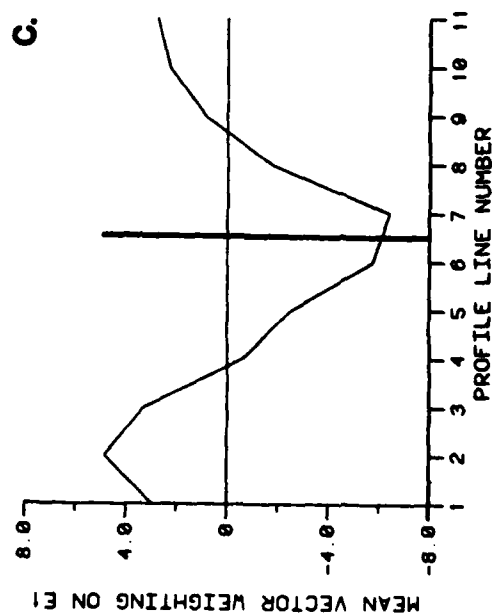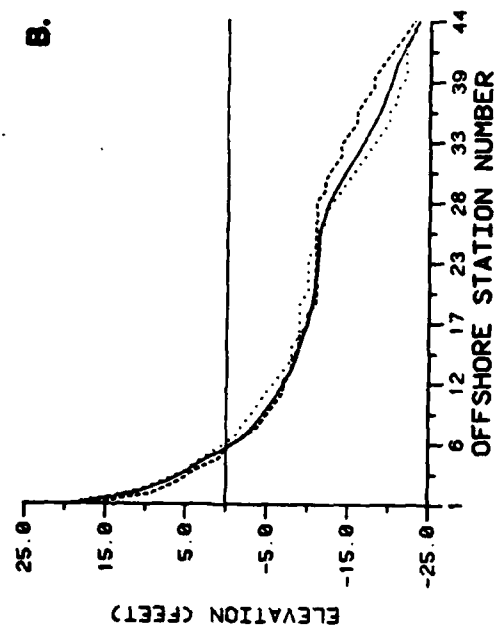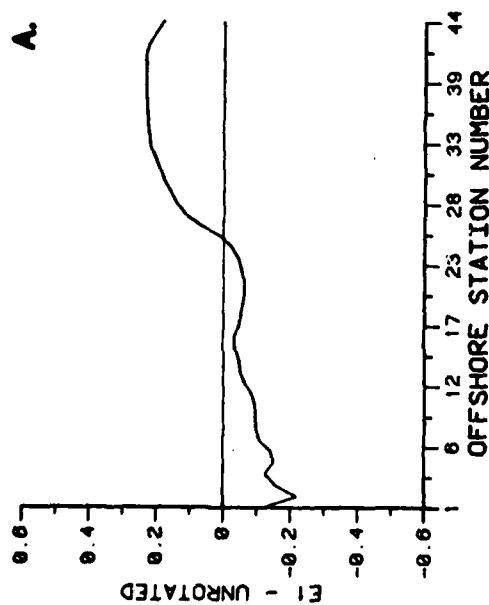
FIGURES 5a - 5d: a)Plotted values for the first vector (E1); b) Reconstructed profile for E1 plotted plus the mean (---) and minus the mean (...); c) Mean vector weighting on E1 over all survey dates for each individual profile; d) Mean vector weighting on E1 for all profiles for each survey date.
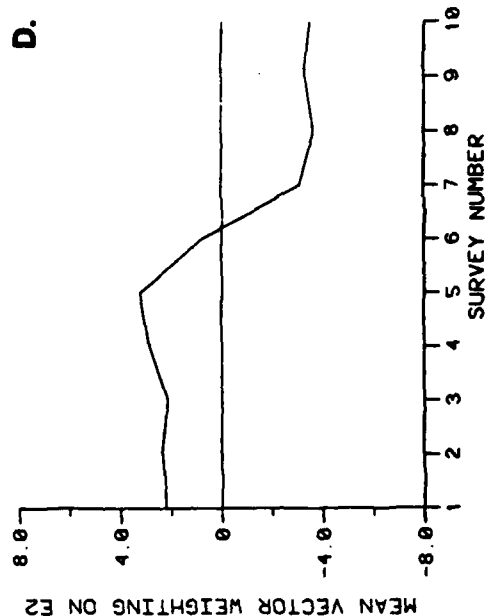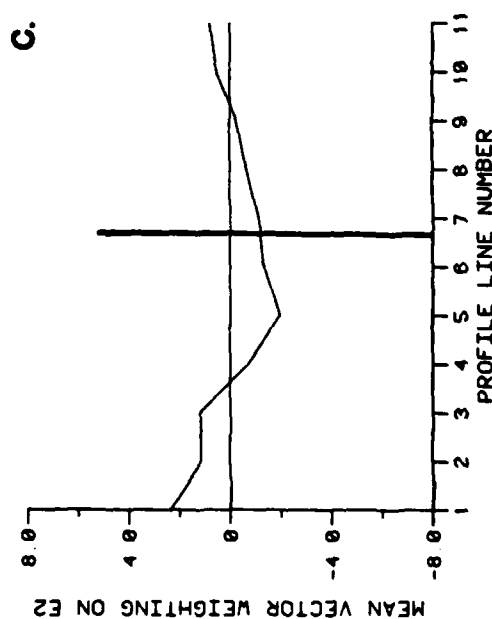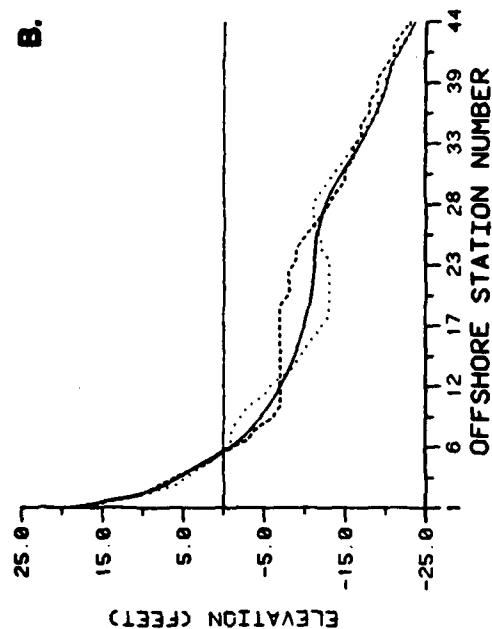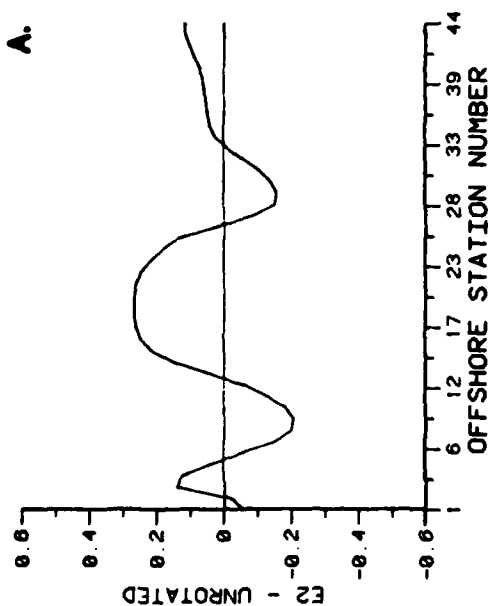
FIGURES 6a – 6d: a) Plotted values for the second vector (E2); b) Reconstructed pro-
file for E2 plotted plus the mean (---) and minus the mean (...);
c) Mean vector weighting on E2 over all survey dates for each in-
dividual profile; d) Mean vector weighting on E2 over all profiles
for each survey date.

-26-
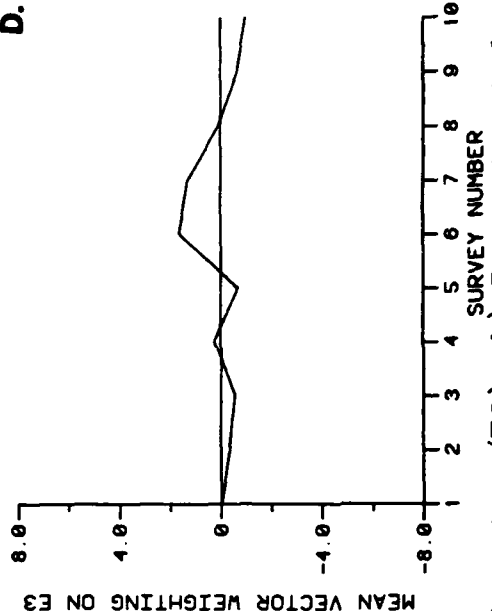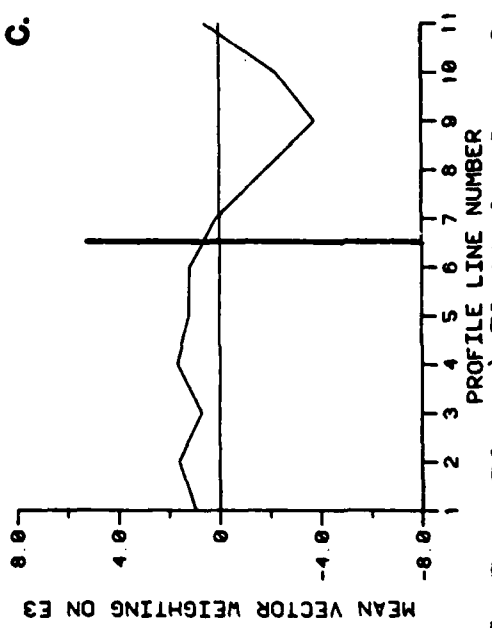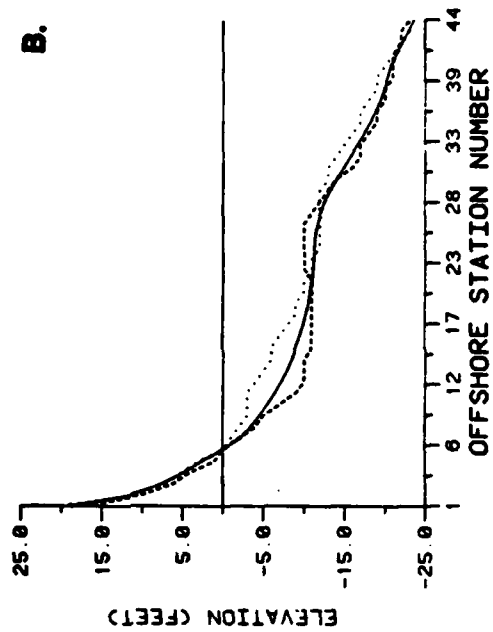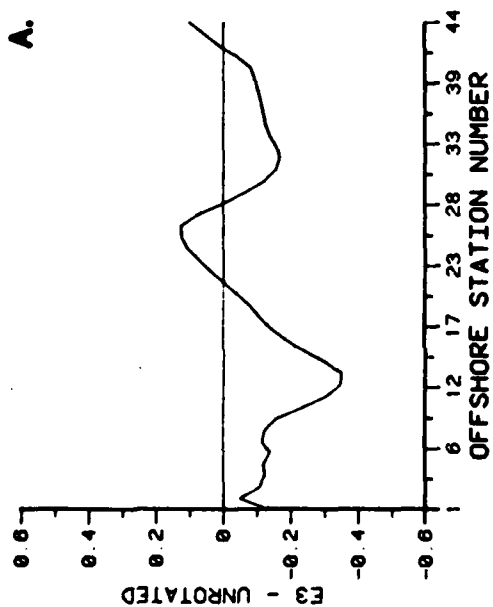
FIGURES 7a - 7d: a) Plotted values for the third vector (E3); b) Reconstructed profile for E3 plotted plus the mean (- - -) and minus the mean (...); c) Mean vector weighting on E3 over all survey dates for each individual profile; d) Mean vector weighting on E3 for all profiles for each survey date.

-27-
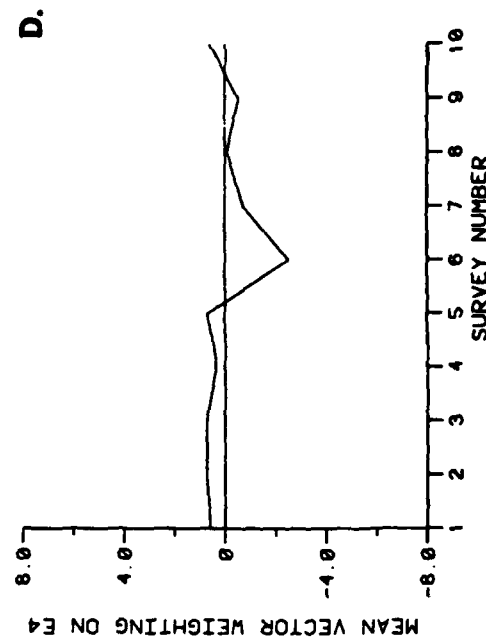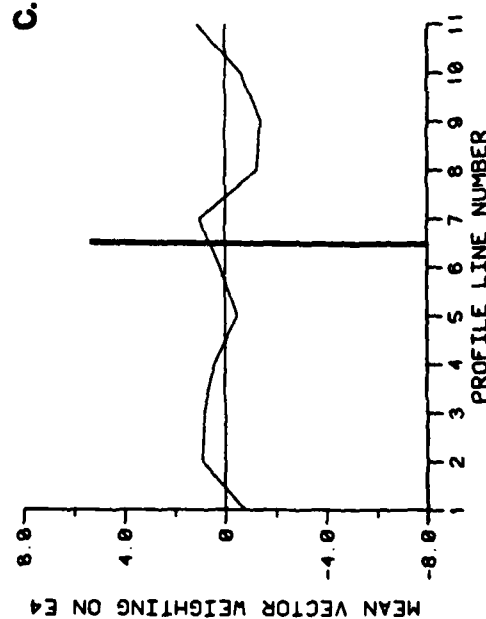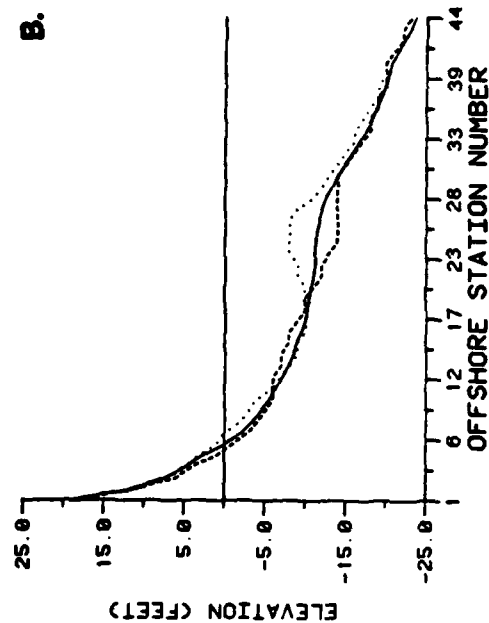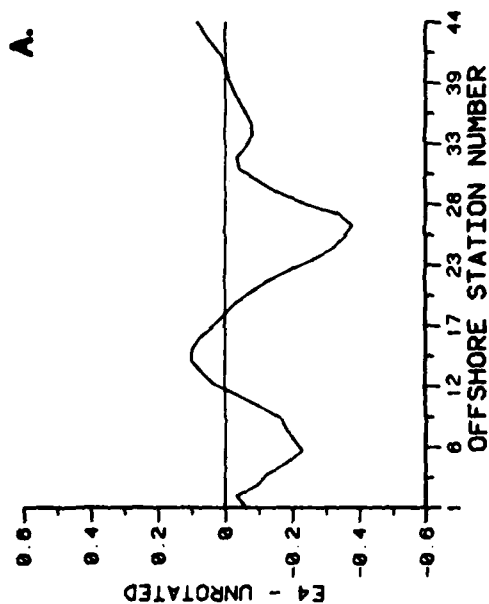
FIGURES 8a – 8d: a) Plotted values for the fourth vector (E4); b) Reconstructed pro-
file for E4 plotted plus the mean (- - -) and minus the mean (...);
c) Mean vector weighting on E4 over all survey dates for each in-
dividual profile; d) Mean vector weighting on E4 for all profiles
for each survey date.

VARIABLE	MEAN	STANDARD DEVIATION	VECTOR 1		VECTOR 2		VECTOR 3		VECTOR 4	
			POS	NEG	POS	NEG	POS	NEG	POS	NEG
1	5.93	.80	6.31	5.55	5.73	6.13	5.48	6.38	6.15	5.71
2	3.52	.55	4.00	3.04	3.43	3.61	3.40	3.64	3.61	3.43
3	2.29	.40	2.55	2.03	2.50	2.08	2.12	2.46	2.45	2.13
4	1.49	.40	1.70	1.28	1.67	1.31	1.29	1.69	1.70	1.28
5	.81	.48	1.10	.52	.87	.75	.58	1.04	1.18	.44
6	0.00	.54	.30	-.30	-.13	.13	-.30	.30	.52	-.52
7	-.67	.54	-.46	-.88	-1.01	-.33	-.93	-.41	-.20	-1.14
8	-1.07	.57	-.89	-1.25	-1.54	-.60	-1.36	-.78	-.63	-1.51
9	-1.40	.64	-1.19	-1.61	-1.94	-.86	-1.81	-.99	-.96	-1.84
10	-1.72	.67	-1.51	-1.93	-2.22	-1.22	-2.36	-1.08	-1.42	-2.02
11	-2.00	.67	-1.81	-2.19	-2.37	-1.63	-2.82	-1.18	-1.88	-2.12
12	-2.24	.65	-2.09	-2.39	-2.41	-2.07	-3.15	-1.33	-2.30	-2.18
13	-2.46	.62	-2.34	-2.58	-2.37	-2.55	-3.33	-1.59	-2.61	-2.31
14	-2.65	.63	-2.52	-2.78	-2.28	-3.02	-3.41	-1.89	-2.89	-2.41
15	-2.80	.68	-2.68	-2.92	-2.22	-3.38	-3.45	-2.15	-3.05	-2.55
16	-2.95	.75	-2.81	-3.09	-2.22	-3.68	-3.50	-2.40	-3.17	-2.73
17	-3.09	.81	-2.90	-3.28	-2.25	-3.93	-3.54	-2.64	-3.21	-2.97
18	-3.20	.85	-2.97	-3.43	-2.30	-4.10	-3.56	-2.84	-3.22	-3.18
19	-3.29	.85	-3.04	-3.54	-2.39	-4.19	-3.55	-3.03	-3.20	-3.38
20	-3.35	.81	-3.09	-3.61	-2.50	-4.20	-3.47	-3.23	-3.12	-3.58
21	-3.42	.76	-3.19	-3.65	-2.64	-4.20	-3.42	-3.42	-3.05	-3.79
22	-3.47	.71	-3.27	-3.67	-2.78	-4.16	-3.35	-3.59	-2.94	-4.00
23	-3.50	.68	-3.34	-3.66	-2.91	-4.09	-3.28	-3.72	-2.80	-4.20
24	-3.53	.65	-3.44	-3.62	-3.06	-4.00	-3.23	-3.83	-2.71	-4.35
25	-3.56	.63	-3.55	-3.57	-3.21	-3.91	-3.22	-3.90	-2.68	-4.44
26	-3.64	.56	-3.80	-3.48	-3.56	-3.72	-3.33	-3.95	-2.80	-4.48
27	-3.75	.50	-4.00	-3.50	-3.90	-3.60	-3.57	-3.93	-3.08	-4.42
28	-3.92	.52	-4.24	-3.60	-4.21	-3.63	-3.89	-3.95	-3.44	-4.40
29	-4.14	.53	-4.51	-3.77	-4.44	-3.84	-4.26	-4.02	-3.82	-4.46
30	-4.38	.54	-4.80	-3.96	-4.64	-4.12	-4.62	-4.14	-4.17	-4.59
31	-4.64	.55	-5.09	-4.19	-4.83	-4.45	-4.97	-4.31	-4.55	-4.73
32	-4.91	.58	-5.41	-4.41	-5.00	-4.82	-5.27	-4.55	-4.83	-4.99
33	-5.17	.62	-5.73	-4.61	-5.14	-5.20	-5.53	-4.81	-5.01	-5.33
34	-5.42	.68	-6.03	-4.81	-5.29	-5.55	-5.76	-5.08	-5.20	-5.64
35	-5.66	.71	-6.31	-5.01	-5.48	-5.84	-5.98	-5.34	-5.45	-5.87
36	-5.87	.69	-6.51	-5.23	-5.67	-6.07	-6.17	-5.57	-5.72	-6.02
37	-6.05	.66	-6.67	-5.43	-5.85	-6.25	-6.31	-5.79	-5.95	-6.15
38	-6.20	.61	-6.77	-5.63	-6.00	-6.40	-6.42	-5.98	-6.15	-6.25
39	-6.33	.54	-6.83	-5.83	-6.15	-6.51	-6.51	-6.15	-6.25	-6.34
40	-6.44	.47	-6.88	-6.00	-6.27	-6.61	-6.58	-6.30	-6.32	-6.43
41	-6.67	.33	-6.97	-6.37	-6.53	-6.81	-6.71	-6.43	-6.45	-6.65
42	-6.90	.23	-7.10	-6.70	-6.79	-7.01	-6.88	-6.92	-6.69	-6.86
43	-7.12	.16	-7.25	-6.99	-7.04	-7.20	-7.08	-7.16	-6.94	-7.08
44	-7.08	.10	-7.07	-7.09	-7.06	-7.10	-7.03	-7.13	-7.09	-7.07

TABLE 6 : Values of means, standard deviations and $\pm 4\,(sd_i)\,(E_{ij})$ added to the mean profile, for the first four eigenvectors.

The average case loading Δ_k for the jth eigenvector at the tth CRAB survey over all profile locations (k) is given by

$$\Delta_k = \frac{1}{11} \sum_{k=1}^{11} E_{ijt}$$

at each survey date t, for j = 1 to 4. These case loadings are shown in Fig. 5d, 6d, 7d, and 8d.

The first eigenvector (E1) explained 35.4% of the total variance and represented the dominant mode of profile variations from the mean. A positive case weighting on E1 indicates a deficiency of sediment on the beach face out to 300 m from the baseline (Fig. 5a). Seaward of this point, there is a surplus of sediment. A negative case weighting on E1 indicates more sediment in the inshore region and less in the offshore area. E1 is a profile rotation function with positive weightings when the profile is flatter than the mean, and negative when steeper. While it was tempting to attribute the along-the-shore variation in mean E1 weightings (Fig. 5c) to the presence of the pier (Miller et al., 1983), the along-the-coast distance between the maximum weighting at profile line number 2 to the minimum at number 7 was 343 m; and Vincent (1973) showed that crescentic sand waves with wave lengths of 140 to 650 m are common along the North Carolina coast. The meanders in the crescentic bar forms were slightly skewed to the north as were the mean

loadings on E1 calculated in this study. This study did not affix cause, only association; and it is clear that along-the-coast profile slope variations at this length scale do occur.

The time history of E1 case loadings for the average profile location is shown in Fig. 5d. Positive values occurred from the first through the fifth survey. After the fifth survey (September 19, 1981), negative weightings prevailed. The transition from a relatively steep to a flatter profile slope was abrupt.

The second eigenvector (E2) (Fig. 6a) explained 25.7% of the total variance. A positive weighting on E2 indicates a single offshore bar at 250 m (Fig. 6b). A negative weighting indicates a seaward displacement of sediment, the development of an inner bar 140 m from the baseline, and an outer bar at 360 m.

The maximum average loading on E2 over all survey data was located on profile line number 1, north of the pier (Fig. 6c). Average loadings declined from this profile line, then increased again on the south side of the pier. There was a tendency for the single-bar configuration to occur at the northern and southern ends of the study site and for the double-bar configuration to occur in the center of the reach. The spatial scale of this variation suggested an along-the-coast variability greater than several km.

The temporal history of the vector loadings (averaged over all profile locations) (Fig. 6d) indicated a change from the single-bar system prior to the 6th survey (November 3rd) to the double-bar configuration thereafter. As was the case with E1, the transition in temporal loadings on E2 was abrupt and occurred between September and November.

The third eigenvector (E3) (Fig. 7a) accounted for 13.1% of the total variance. A positive weighting on E3 indicates a bar 290 m from the baseline, a broad, deep inner trough and less sediment on the beach face (Fig. 7b). A negative weighting indicates buildup of the beach face, a broad inner bar, and a surplus of sand seaward of 360 m.

The mean loading on each profile for E3 was positive, except on three profiles to the south of the pier (Fig. 7c). The time history of E3 was marked by a period of positive loadings which occurred simultaneously with the changes in E1 and E2 (Fig. 7d).

Eigenvector four (E4) (Fig. 8a) explained 10.2% of the total variance. A positive weighting on E4 indicates an inner bar 200 m from the baseline and a deficiency of sand along the remainder of the profile, except for the extreme offshore region seaward of 500 m (Fig. 8b). A negative weighting indicates a sand surplus at the beach face, a well-developed outer bar located approximately 300 m from the baseline, and a trough in between.

The spatial variations in E4 were small (Fig. 8c). The majority of the profiles to the north of the pier were positively weighted, whereas the southern profiles were negatively weighted. The time series of the E4 loadings (Fig. 8d) were very significant. The weightings were positive on E4 through the September 19, 1981, survey, after which the weightings became negative. This coincided with the major shifts in the other three vectors.

Storms and Profile Changes

During the study period three different storm types occurred: hurricanes/tropical storms, extratropical cyclones and anticyclones. Table 2 summarizes the important parameters of the six individual storm events.

Hurricane Dennis and Tropical Storm Emily caused only minor changes in the FRF bathymetry. Dennis caused variation only on profiles 4 and 6 (as is evidenced in the E1-E2 plots, Fig. 9-10). The effects on the two profiles were opposite: positive on 4 and negative on 6. Tropical Storm Emily caused sufficient changes on several profiles to significantly alter the mean profile for the September 19, 1981, survey (Fig.4). The beginning of a small offshore bar appeared in this survey.

Two high pressure systems occurred in October, 1981. generating high winds and waves at the pier. During this month, large changes were made in the local bathymetry. The

-33-
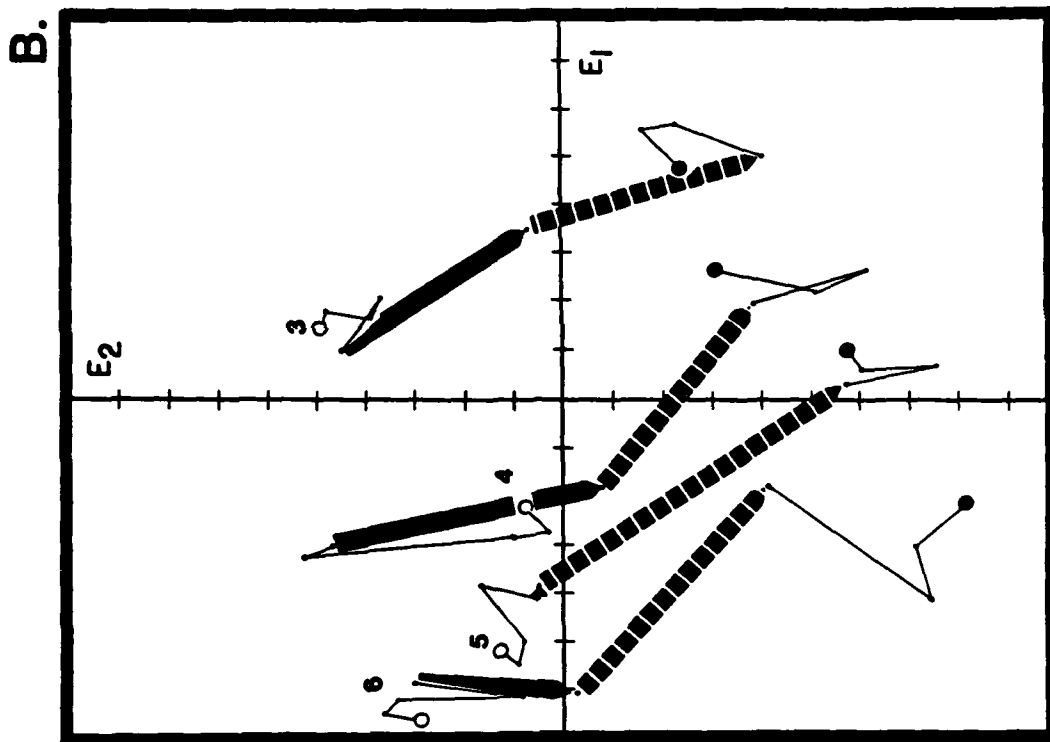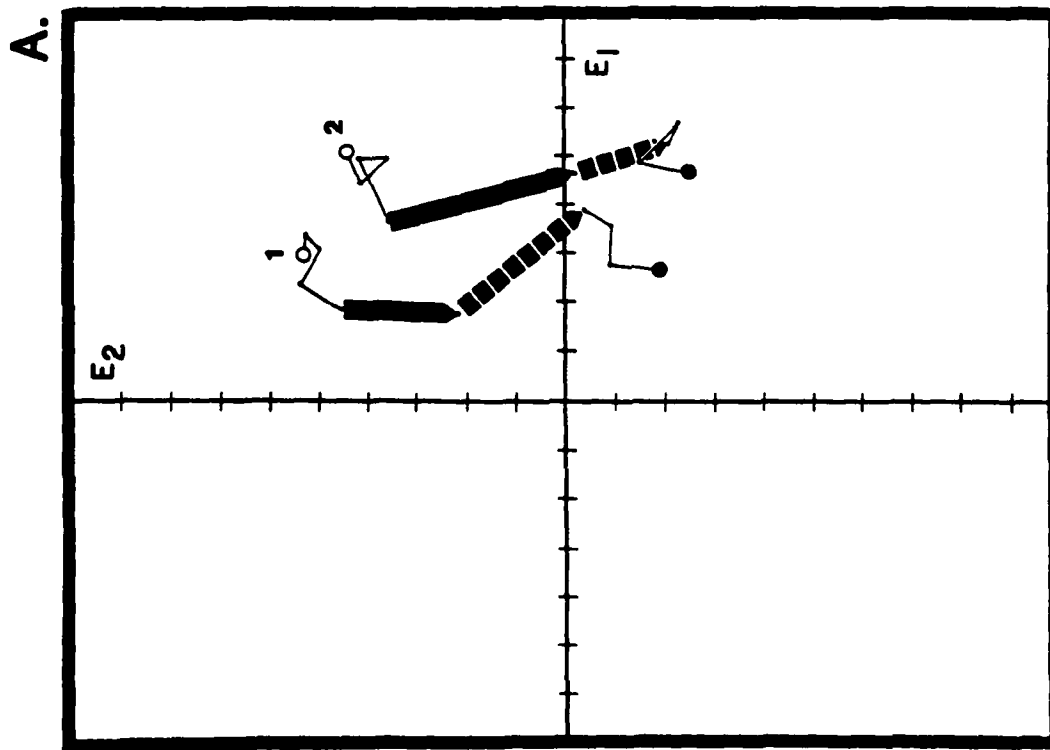
FIGURES 9a - 9b: Profile lines 1 through 6 plotted in E1-E2 eigenvector space. Explanation of symbols used in Fig. 9 and 10 may be found in Table 8.
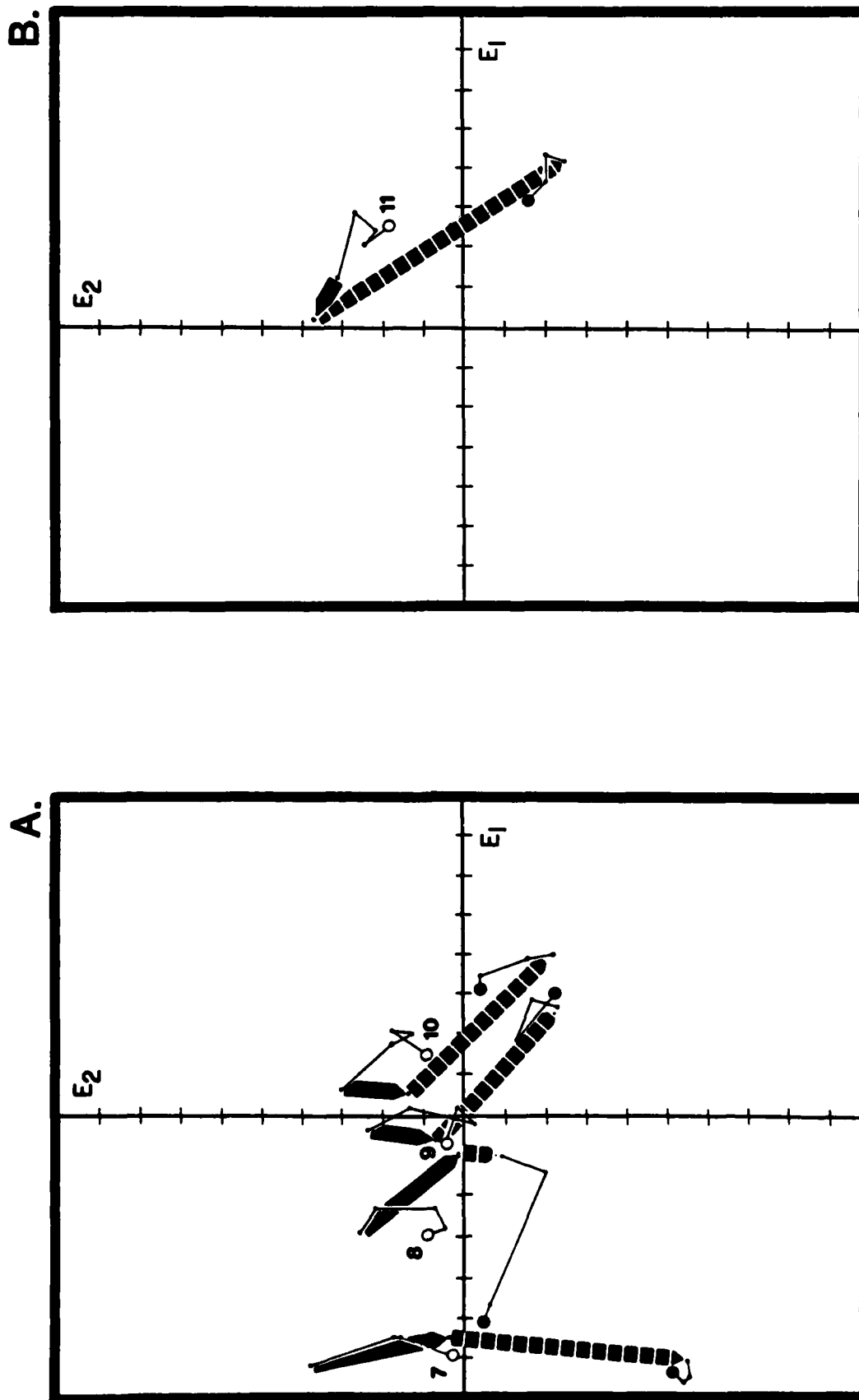
FIGURES 10a - 10b: Profile lines 7 through 11 plotted in E1-E2 eigenvector space.

largest changes in E3 and E4 were also observed during this period, along with the second largest variations in E1 and E2. The morphological responses to these changes were offshore sediment movement and the development of the storm bar approximately 300 m from the FRF baseline.

During November, the two extratropical cyclones that skirted the mid-Atlantic coast made additional changes in the profiles. The first storm caused large changes in E1 and E2 and smaller changes in E3 and E4. This storm moved the storm bar 60 m farther offshore and further developed the inner bar. The second storm continued the development of storm profile features.

Profile Form and Profile Changes

Two survey periods (September 19, 1981, to November 3, 1981; and November 3 to November 16) were analyzed to answer questions about the importance of original profile form on subsequent profile change. The bulk of the profile changes during the study period occurred during these surveys. These changes were analyzed by plotting the loading on a vector at one survey date against the change in the vector loading at the next survey. The graphs (Fig. 11 and 12) indicated onshore-offshore movement of sediment (E1 vs ΔE1) and the development of bars on the profile (E2 vs ΔE2). Linear regression was used to assign a degree of correlation and significance to the relationship.
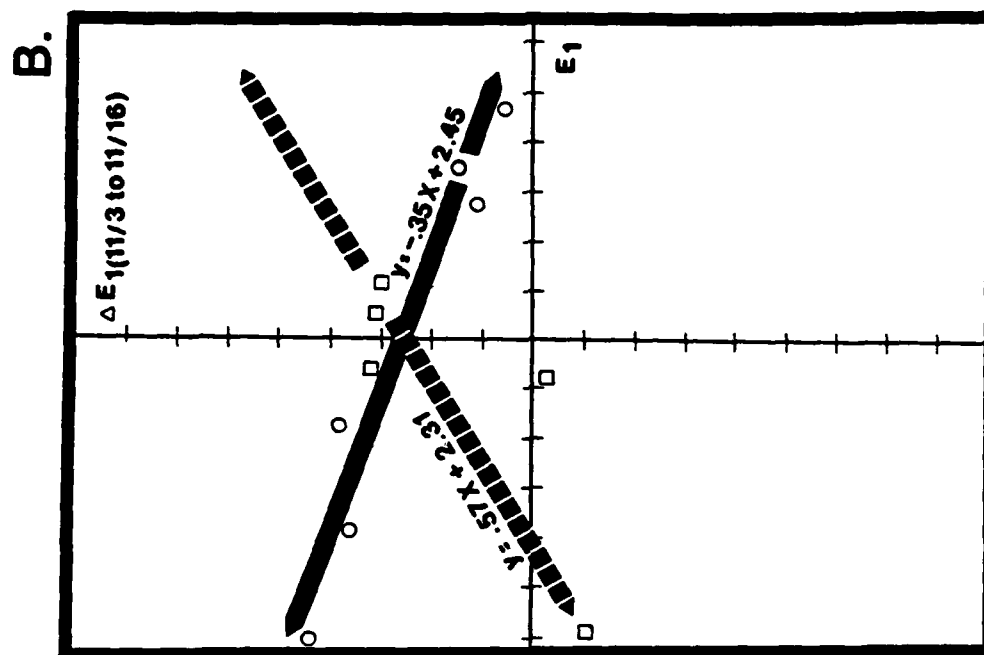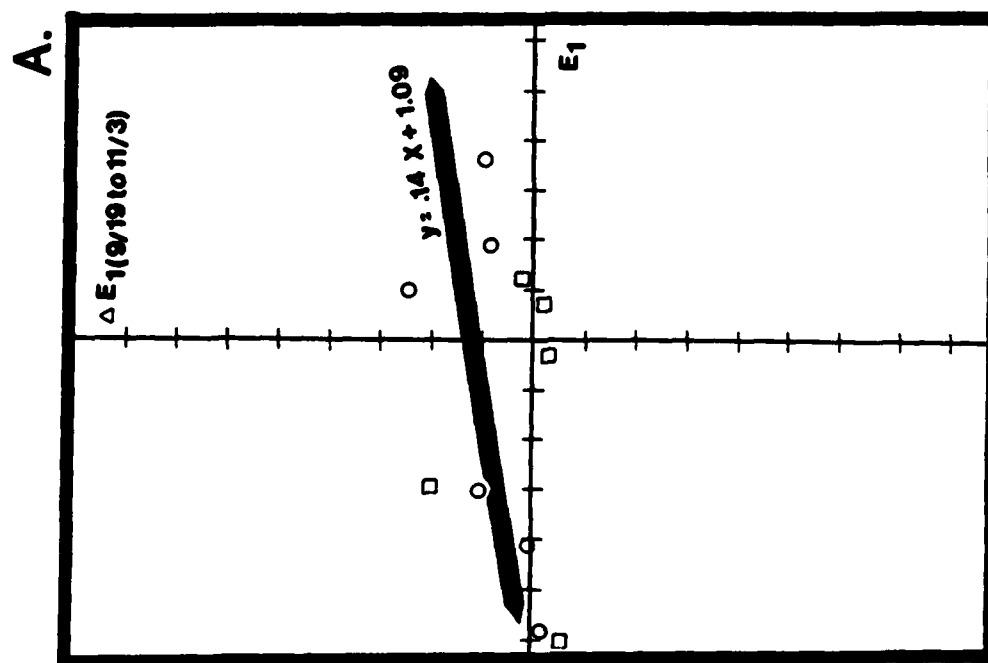
FIGURES 11a - 11b: a) Changes in E1 between surveys 5 and 6, versus the vector loadings for survey 5; b) Changes in E1 between surveys 6 and 7, versus the loadings for survey 6. Open circles and squares indicate points located to the north and south of the pier, respectively. Heavy solid and heavy dashed lines are regression lines for points north and south of the pier, respectively.
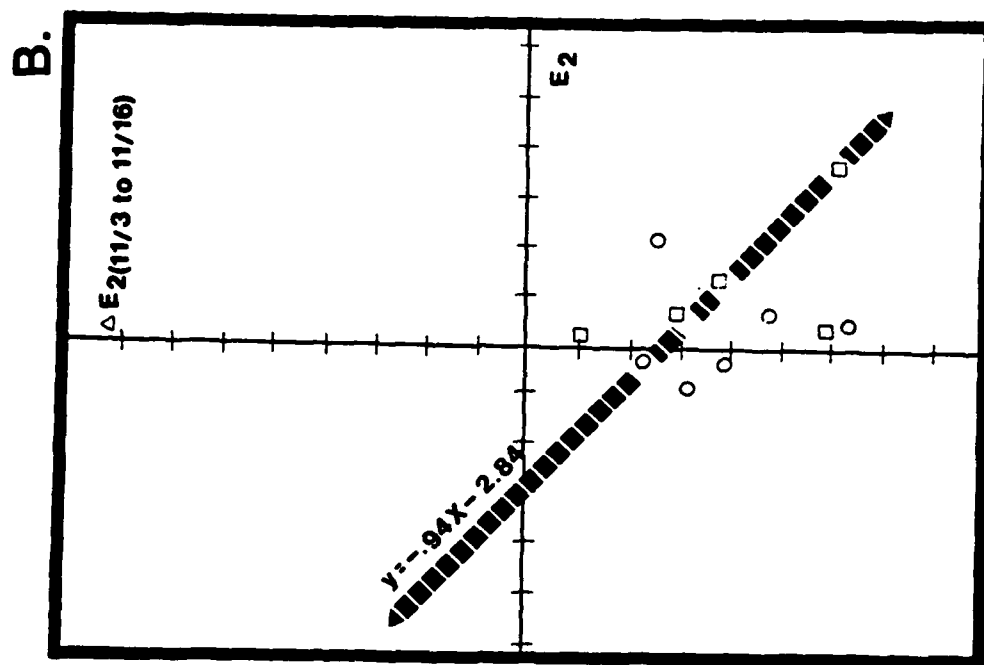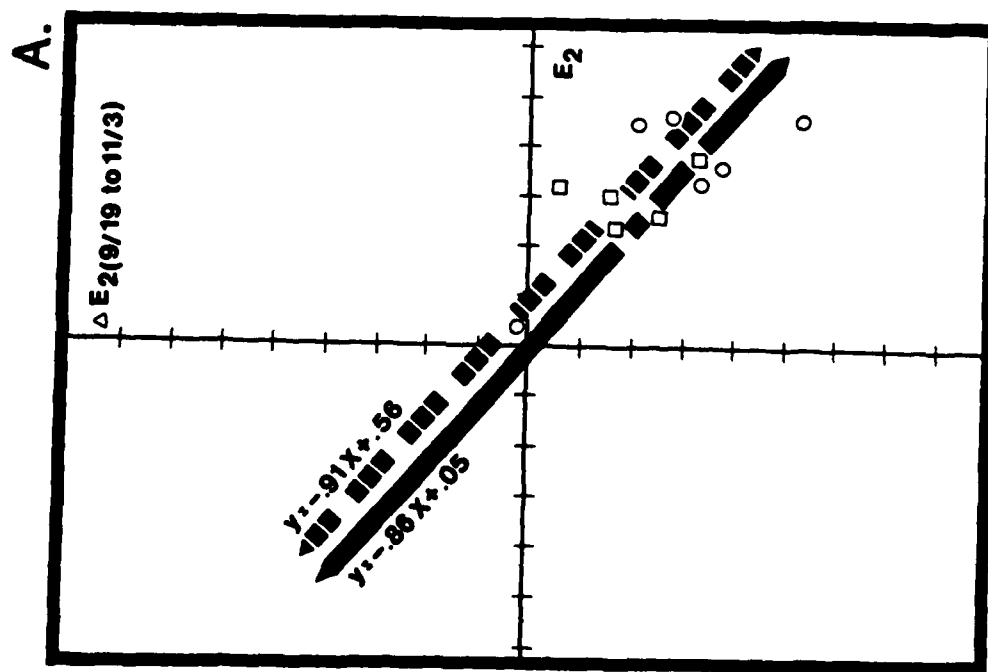
FIGURES 12a - 12b: a) Changes in E2 between surveys 5 and 6, versus the vector
loadings for survey 5; b) Changes in E2 between surveys 6 and 7,
versus the loadings for survey 6. Open circles and squares in-
dicate points located to the north and south of the pier, respec-
tively. Heavy solid line, dashed line and broken dashed line are
regression lines for points north of the pier, south of the pier
and for both sides of the pier, respectively.

Fig. 11a shows the changes in E1 during October as a function of E1 at the beginning of the period. This was the period in which two high pressure systems were responsible for two large wave events. The mean profiles showed positive changes in E1 for increasing values of E1 at the beginning of the period. A positive change in the weightings on E1 indicates offshore sediment movement, while a negative change indicates onshore sediment movement. The north-of-pier profiles had a (E1 vs ΔE1) correlation coefficient of .593 (α_{95} = .11). Thus, the flatter the profile, the greater is the subsequent offshore sediment movement, further flattening the profile. The changes in E1 for the period spanning the occurrence of the two cyclones of November are shown in Fig. 11b relative to the weighting on E1 at the beginning of the period. The correlations between E1 and ΔE1 for the areas to the north and south of the pier were -.965 (α_{95}=.0009) and +.832, (α_{95} = .04), respectively. South of the pier, offshore displacement of sediment was greater in areas with flatter profiles prior to the survey period. The opposite relationship prevailed north of the pier.

Fig. 12 shows the changes in E2 relative to E2 at the beginning of the period of high pressure systems in October. Negative weightings on E2 indicate the tendency for a double-bar profile. Profiles with a more highly developed original single-bar configuration showed a greater tendency

to change toward a double-bar configuration. The north-of-pier data points had a correlation coefficient of -.760, and the combined data points showed a correlation of -.650 (α_{95}=.02). The changes in E2 during the passage of the extratropical cyclone in November showed negative displacement, indicating storm profile development (Fig. 12b). The changes were greater for this latter period than in the earlier period. The south-of-pier data points showed a correlation coefficient of -.641 (α_{95}=.12). From this we inferred that for both the October high pressure period and the November cyclone period, the change toward two bars was most extreme where the single-bar form was most highly developed.

The relationship between E2 for a survey and the subsequent change in E2 was analyzed for each survey interval (Fig. 13 and Table 7). A statistically significant relationship was found for all those intervals in which storms occurred. In each case the slope of the relationship was negative. Apparently the slope is a reflection that incident wave energy from storms was applied in these periods, work was done on the sedimentary prism, and large E2s resulted. The x-intercept indicates the equilibrium E2 weighting for the period. For the period that included Hurricane Dennis the equilibrium value of E2 was 3.3. Profiles prior to Dennis with E2s greater than 3.3 had a decline in E2 during the period while those profiles with an
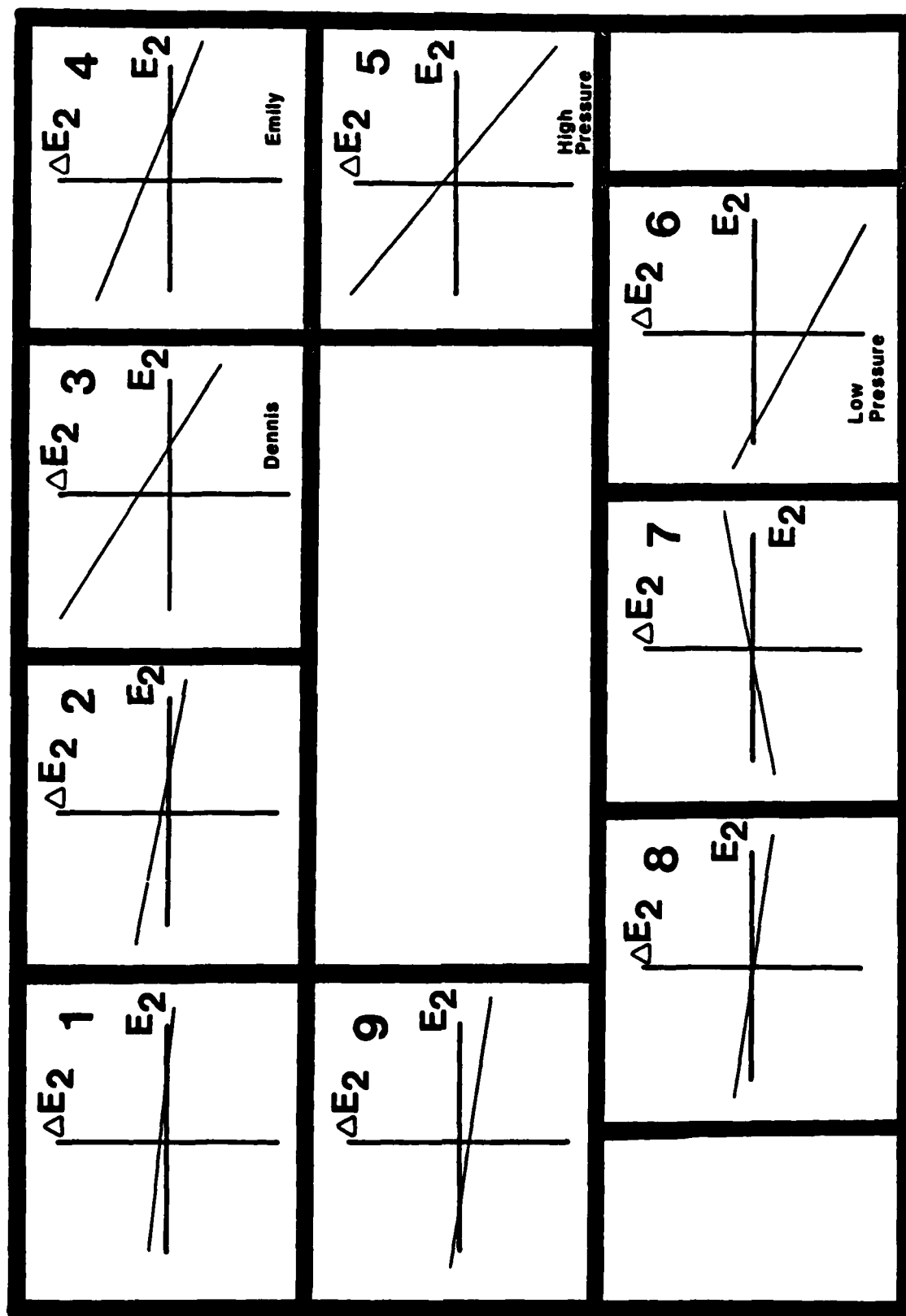
FIGURE 13:   Regression lines for correlations between the weightings on E2 and the change in E2 between survey periods.

SURVEY NUMBER	CORRELATION	X-INTERCEPT	Y-INTERCEPT	SIGNIFICANCE
1	-.10803	6.27	0.20	.37594
2	-.67973	1.10	0.18	.01071
3	-.52681	3.34	1.84	.04795
4	-.63866	3.73	1.67	.01721
5	-.69136	0.78	0.78	.00923
6	-.38890	-6.39	-3.48	.11859
7	+.23303	-0.46	0.09	.24523
8	-.31488	-1.13	-0.16	.17281
9	-.28551	5.15	-0.55	.19737

TABLE 7 : Statistics associated with the regression lines in FIGURE 13.

E2 less than 3.3 had an increase in E2 over the period. For the survey spanning tropical storm Emily the equilibrium E2 weighting was 3.7. For the period of the two high pressure systems in October the equilibrium condition was 0.8, similar to the grand mean profile but with a greater amplitude in the single-bar-and-trough configuration. In the November storm period the equilibrium point for E2 was -6.4. The two-bar profile was the equilibrium condition. The current study was not designed to answer the question of the cause of a particular equilibrium "setting" for E2, but we will offer some speculation in the discussion section.

Profile Changes In E1-E2 and E3-E4 Space

At each survey date, each profile may be represented as a point in eigenvector space. The results of the analysis in E1-E2 space are shown in Table 8 and Fig. 9, 10 and 14. For E3-E4 space the results are shown in Fig. 15 and 16. A plot of the temporal weightings on E1 and E2 (E3 and E4) in a cartesian coordinate system shows the nature of change in profile shape between survey dates. The length of the individual line segments connecting these points is a measure of the magnitude of change in profile morphology between surveys. By these plots the periods of maximum profile change at the FRF can be easily identified. To better understand these sediment movements in eigenvector space, the characteristic profile for the four cartesian

	: July 2, 1981
	: July 17, 1981
	: August 4, 1981
	: August 24, 1981
	: September 19, 1981
	: November 3, 1981
	: November 16, 1981
	: January 5, 1982
	: February 9, 1982
	: March 18, 1982

TABLE 8 :   Summary of symbols used in FIGURES 9, 10, and
15a through 15k.
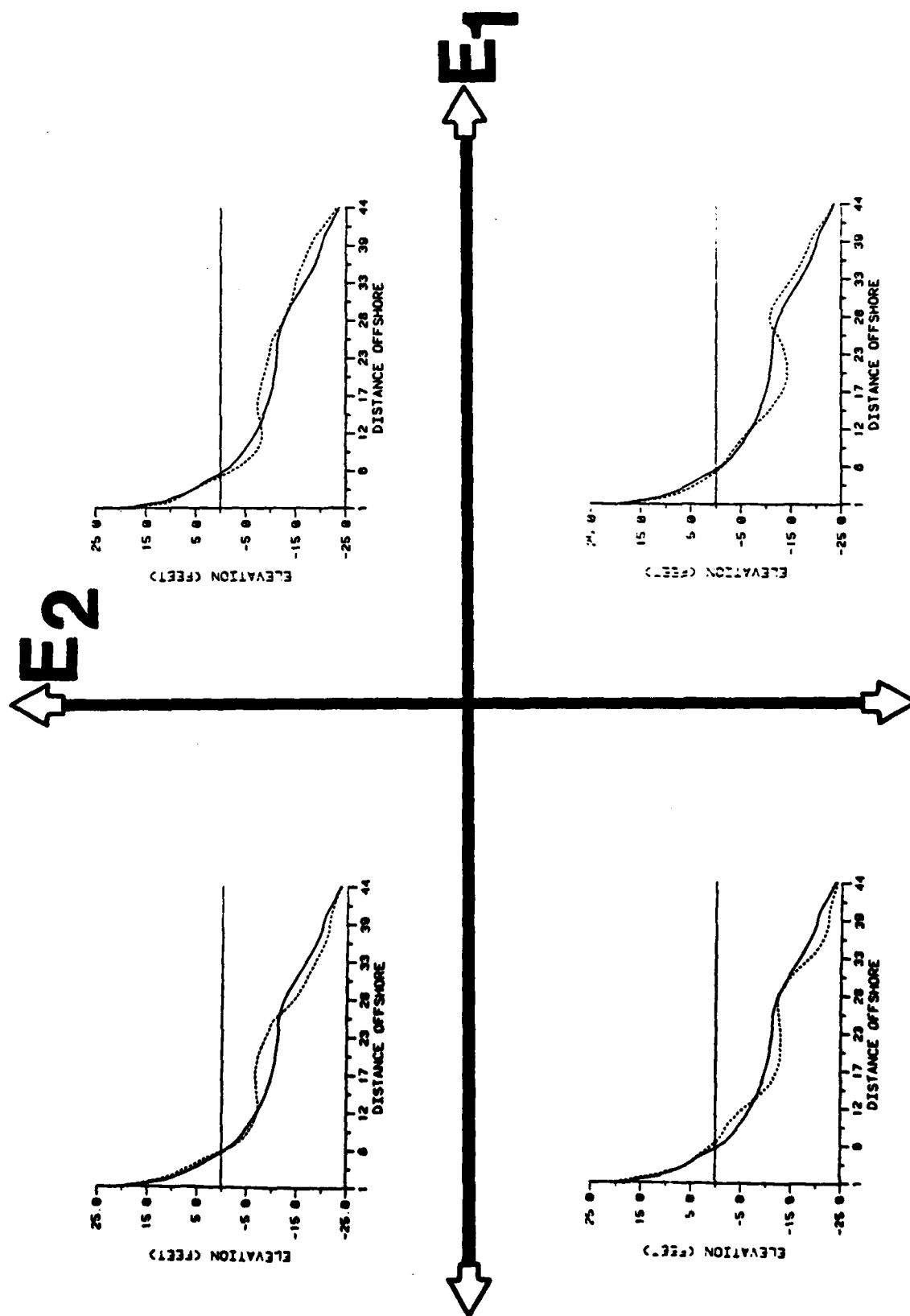
FIGURE 14: Characteristic profiles in each of the cartesian quadrants for the plots in E1-E2 eigenvector space.
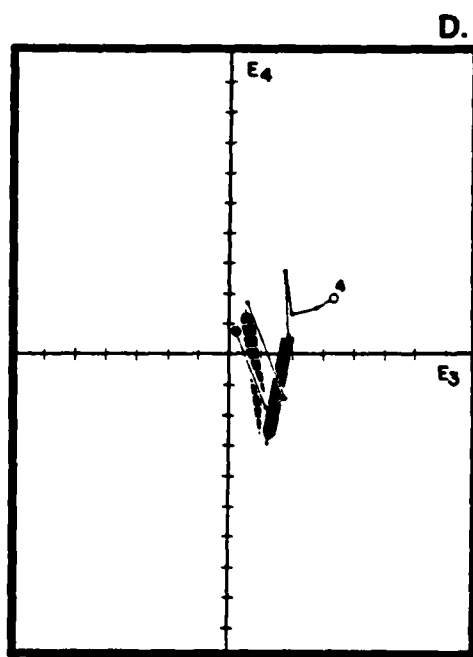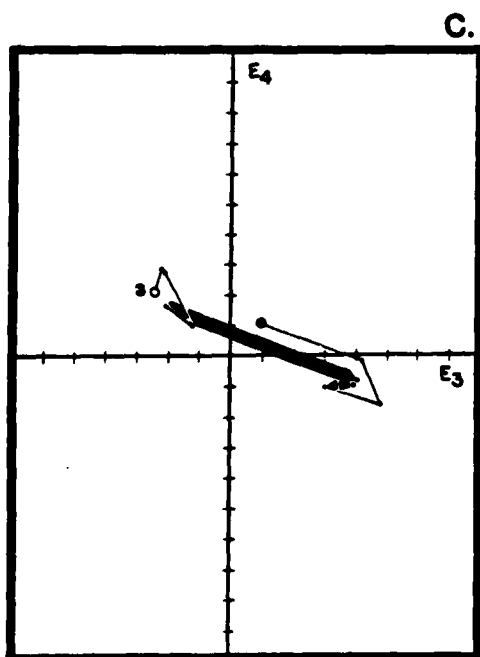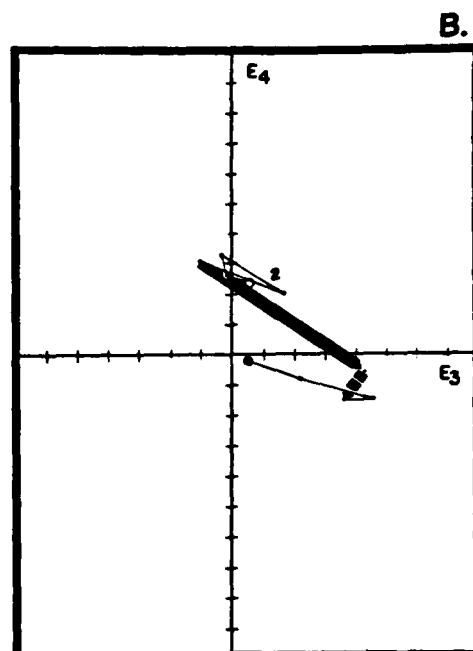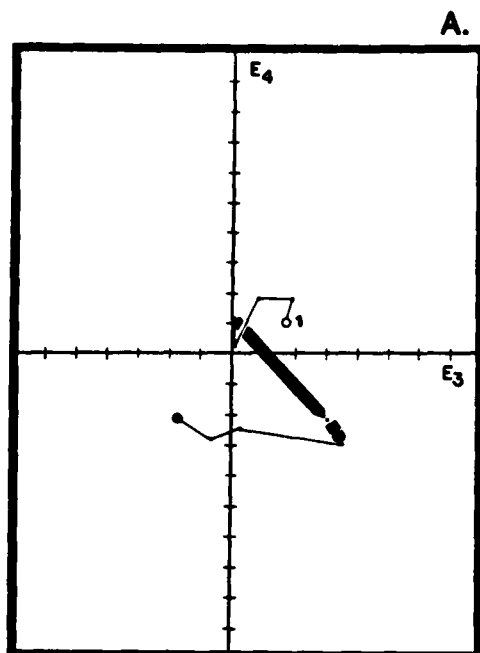
FIGURES 15a - 15d: Profile lines 1 through 4 plotted in E3-E4 eigenvector space.

-46-
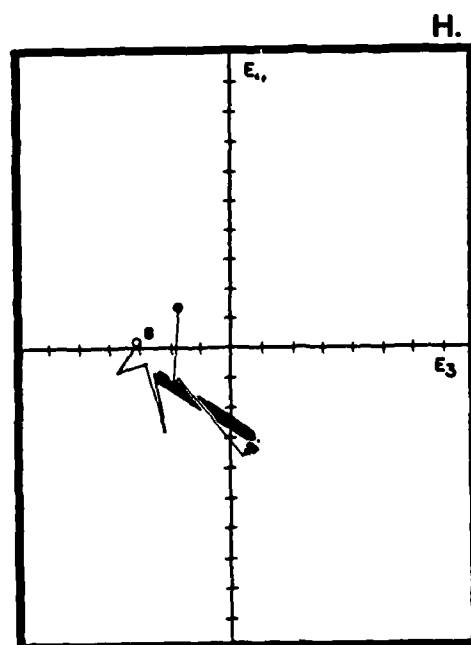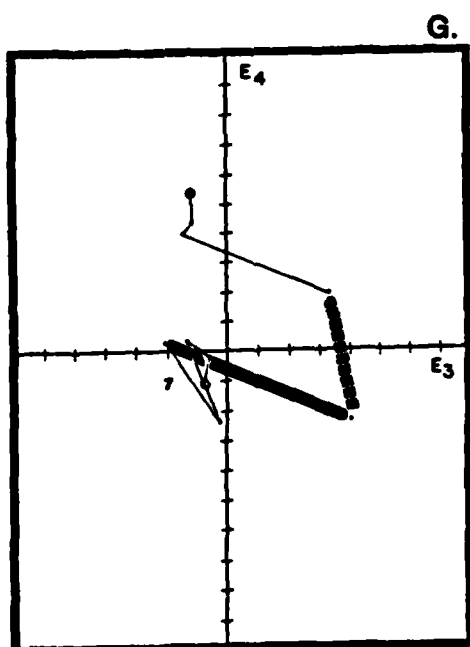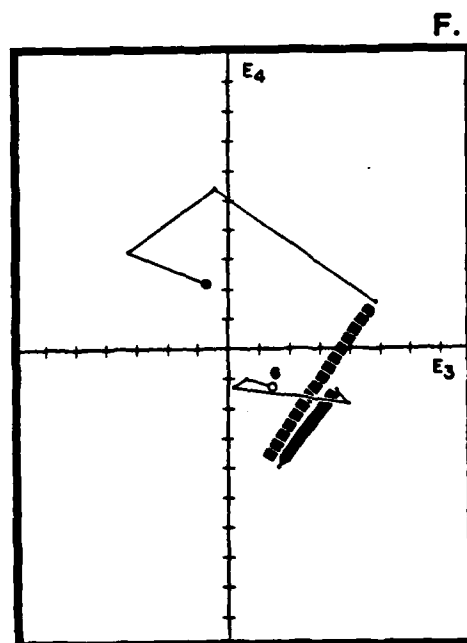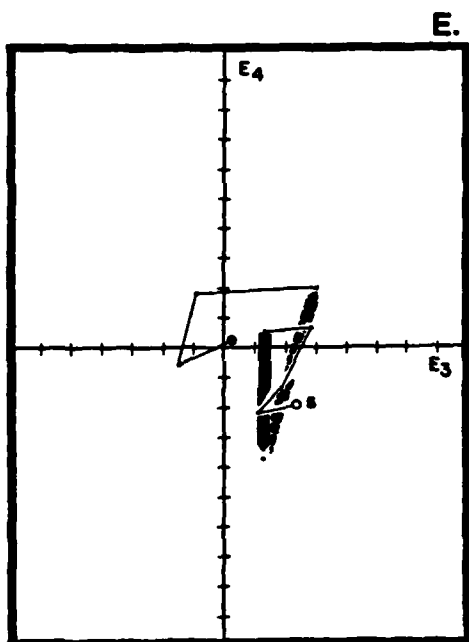
FIGURES 15e - 15h: Profile lines 5 through 8 plotted in E3-E4 eigenvector space.
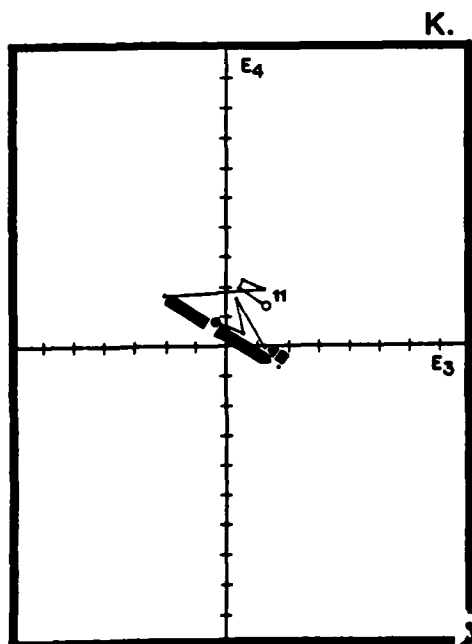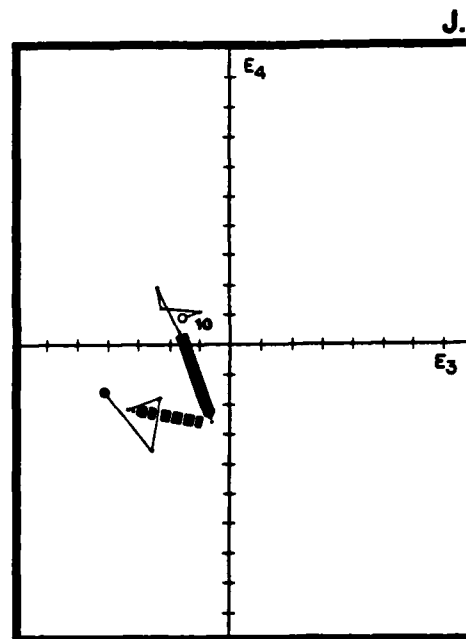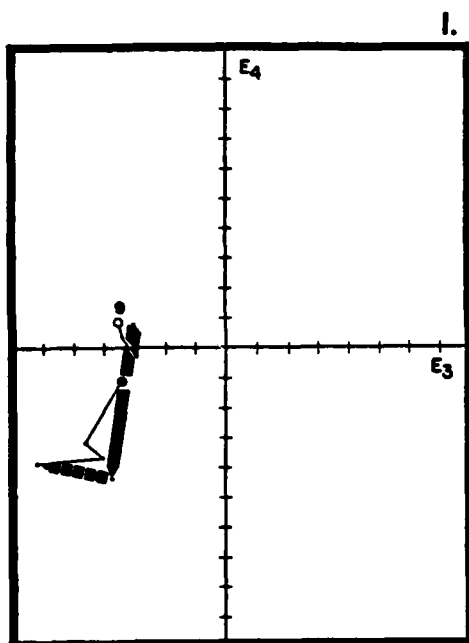
FIGURES 15i - 15k: Profile lines 9 through 11 plotted in E3-E4 eigenvector space.
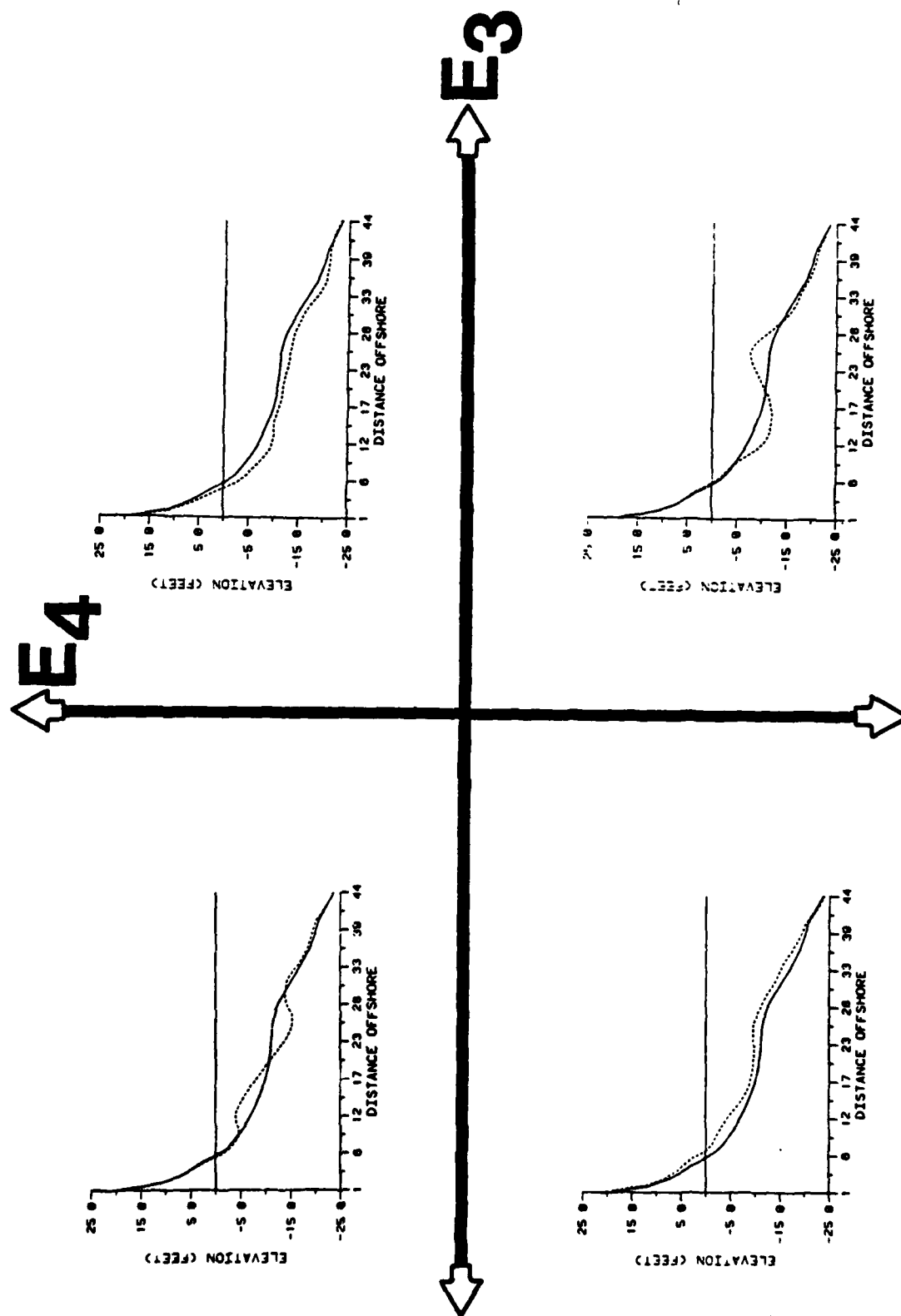
FIGURE 16: Characteristic profiles in each of the cartesian quadrants for the plots in E3-E4 space.

quadrants is reconstructed as follows:

$$\bar{R}_{ij} = \bar{X}_i + (\pm C)(SD_i)(E_{ij}) + (\pm C)(SD_i)(E_{ij})$$

where $\bar{R}_{ij}$ is the reconstructed value for the ith point along the profile of the jth eigenvector. $\bar{X}_i$ is the mean profile elevation at the ith point along the profile. $\pm C$ is a constant which is representative of the case loadings on a particular vector. The sign is dependent upon the cartesian quadrant being reconstructed. SD_i is the standard deviation of the profile elevation at the ith point along the profile, and E_{ij} is the loading on the jth eigenvector for the ith point along the profile (Fig. 14 and 16). These reconstructed profiles for each quadrant demonstrate the meaning of various points in eigenvector space.

The passage of Hurricane Dennis (between the August 4 and August 24 surveys) caused substantial changes in only two FRF profile lines (numbers 4 and 6). Both of these profile lines were located on the north side of the pier. Profile line number 4 experienced large positive movements while line number 6 showed large negative movements. Profile line numbers 3 and 6 were the only profile lines to show a negative movement along E2 during the period. The remaining profile lines showed positive movement along the E2 axis; however, most of these were small increments.

The September 19 to November 3 survey period showed smaller changes on all profiles except profile line number

5. These changes are denoted by the heavy solid lines in Fig. 9 and 10. All profile lines except number 11 showed large negative tendencies in the E2 direction with very little variance in E1 values. This indicates that bar formation occurs prior to changes in the slope.

In E1-E2 space the greatest change in the morphology occurred between the November 3, 1981, and November 16, 1981, survey dates; and all profile lines, except numbers 2 and 8, showed these changes. This change is shown by the heavy dashed black lines in Fig. 9 and 10. In all cases, the weightings on E2 became negative, indicating change from quadrants I and IV to quadrants II and III. A negative weighting on E2 shows a seaward displacement of sediment and the formation of a double-bar storm profile. During the period, loadings on E1 generally became more positive, indicating offshore displacement of sand. Profile line numbers 1-4 and 9-11 ended in quadrant II after this period with a well developed storm bar 360 m from the baseline and a smaller inner bar 140 m from the baseline. The remaining profile lines (numbers 5-8), which are located in close proximity to the pier, showed a well developed inner bar and a smaller storm bar located in the same locations as on the other profiles. The only difference in the profiles was the relative size of the two-bar forms.

The plots in E3-E4 space also showed large-scale variations in the FRF bathymetry during the October-November

period. The maximum morphological changes on all profile lines (except numbers 4-6) occurred between the September 19 and November 3 surveys. These changes are shown in Fig. 15a-15k by the heavy black lines. All movements were into quadrant II where a storm bar is centered 300 m from the baseline and a small inner bar is welded to the beach face (Fig. 16). These changes appear to designate the initial stages of the storm profile development and the offshore displacement of sediment along the profile.

The largest changes observed between the November 3 and the November 16 surveys occurred in profile line numbers 4-7. These changes, characterized by movements into quadrant I, indicate a net loss of sediment at all profile points and are shown by the heavy dashed lines in Fig. 15a-15k. Values for E4 have large positive increments. For this same period Miller et al. (1983) described large gross changes (the sum of the absolute values of all volumetric changes along a profile) away from the pier, while net changes (the sum of all positive and negative elevational changes) were small. In the vicinity of the pier, net changes were high. They noted a net loss of sediment from the north side of the pier to the south side.

Analysis of Shore-Parallel Transects

The first eigenvector of principal components analysis of the data, organized as a series of shore-parallel

transects, explained 98% of the total variance. The first vector indicates either more or less sand than the mean at all locations along the shore-parallel transect. Because the transects are shore parallel, variance associated with bars and troughs is not present. Only relative elevation between points is shown. None of the higher order vectors met the Overland and Preisendorfer (1982) statistical test, nor did they make geophysical sense. This analysis was also performed on the data separating the north and south sides of the pier. The mean loading for all survey dates was calculated for the jth eigenvector at the ith point along the profile. Each of the 44 mean values (E_{ij}) was then compared to the actual vector loading (E_{ijt}) and the sign of the difference was plotted in Fig. 17, providing a prognostic overview of the time series of sediment displacements. At each distance from the shore the sum of E_{ijt} over all surveys is zero. Thus, the chart shows the variations in the sediment budget over the study period.

In terms of a gross sand budget there was no net aggregate difference for one side of the pier relative to the other. More sand than the average amount was in the subaerial region during surveys 1-6. Sand in this region shifted to less than the average amount during surveys 7-10. The region immediately seaward of the subaerial region, 100 to 175 m from the baseline, had the opposite response. The early surveys showed less sand than the mean, while the
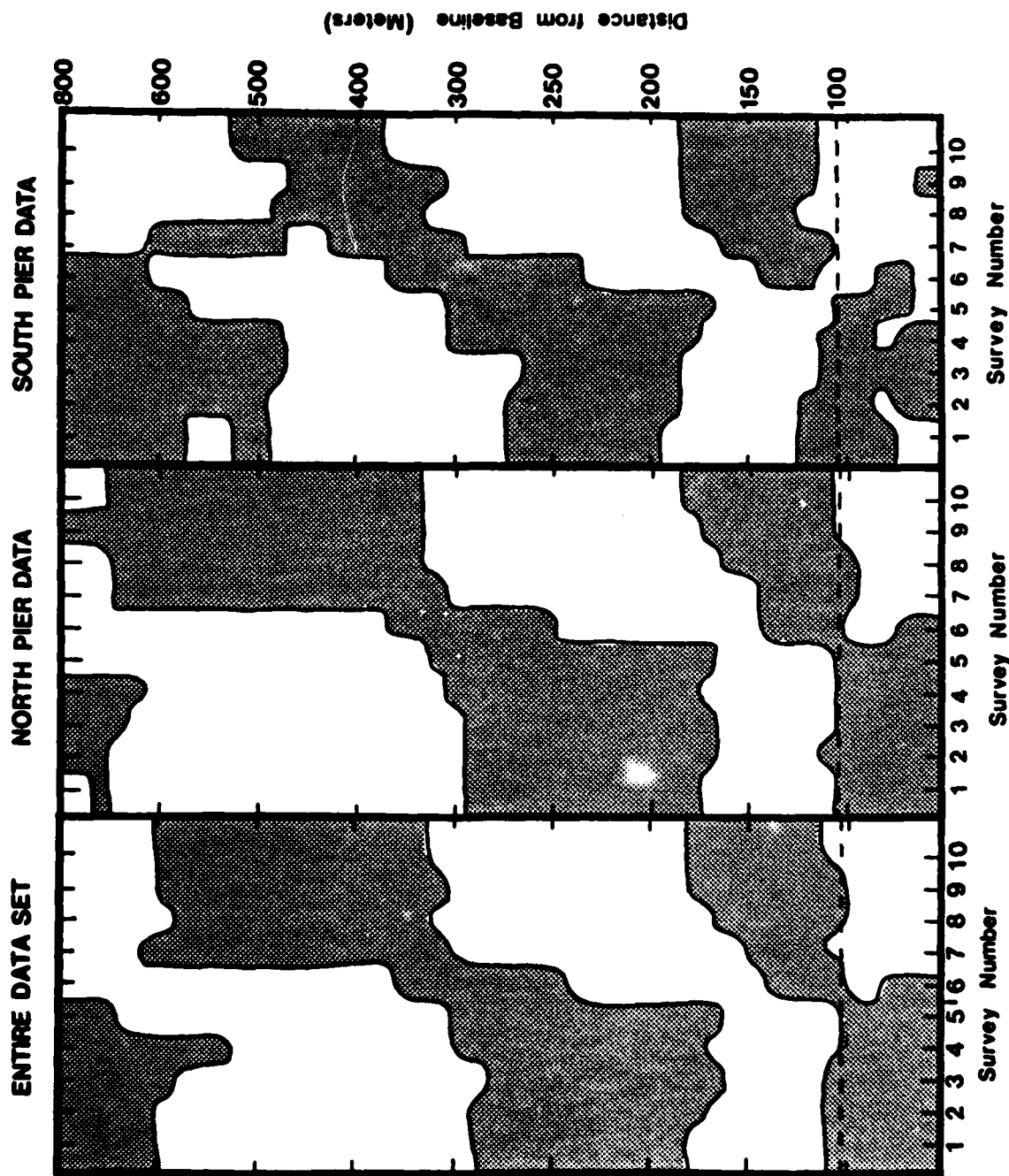
FIGURE 17: Shore-parallel plots showing sand levels greater-or-less than the mean sediment level for both sides of the pier, north of the pier, and south of the pier. Shaded regions indicate areas where the sand level is greater than the mean FRF sediment level.

-54-

later surveys showed more than the mean. We concluded that the sand was shifted from the subaerial region to this region.

Between 175 m and 300 m from the FRF baseline there was a relative sand surplus in the early surveys and a deficit in the later surveys. The apparent recipient of this sand in the later surveys was the zone between 300 and 600 m. In the seaward-most area, 600 to 800 m, there was, again, a sand surplus in the early part of the record and a deficit in later periods. While the profiles do not extend seaward of 800 m from the FRF baseline, it is reasonable to assume that the "missing" sand in the later surveys was transported to some point beyond 800 m from the FRF baseline. The resolution of the data in this region makes the whereabouts of the "missing sand" somewhat questionable, however.

Most of the observed changes occurred between the 5th and the 7th surveys, apparently as a result of the high pressure "storms" of October and the cyclones of November. It is interesting that the exchanges across the shoreline (100 m), across the 300-meter distance, and across some distance seaward of 800 m occurred synchronously. The time of change does not appear to be a function of water depth. This simultaneity suggests shore-normal resonant motions such as edge waves. If this is the case then this shore-parallel form of eigenvector analysis may prove to have been especially useful.

DISCUSSION AND CONCLUSIONS

The summer to winter transition in shorezone morphology is clearly evident in the principal components of the correlation matrix of the FRF shorezone profiles. During this period the shorezone became more dissipative as the profile became flatter and a double-bar configuration replaced the single bar of summer. These changes occurred simultaneously over all water depths. In terms of the bar-and-trough configuration there is apparently an equilibrium form "appropriate" to each storm that occurs. The small differences in the wave characteristics between individual storms were insufficient to account for the variations in bar/trough equilibrium or the observed changes in profile steepness.

Two hurricanes, two anticyclones, and two cyclones occurred during the period of study. Each of these storms generated waves of similar heights (2 to 2.5 m). The two hurricanes produced waves that resulted in nearly identical bar/trough equilibrium forms. Neither hurricane caused changes in profile steepness. The two anticyclones of October caused the profiles to flatten and, for the equilibrium bar/trough configuration, to shift markedly toward a two-bar form. The two cyclones of November produced waves that caused further flattening of the profile and accentuation of the two-bar configuration.

The waves produced during the storms caused adjustments in the bar/trough equilibrium form; whereas, periods without storms showed no evidence of changes in the bar/trough profile. In these analyses the direction of change in the bar/trough equilibrium point was not shown to be directly related to either wave height, wave period, wave direction, wave steepness, breaker type or tidal levels, since all parameters varied very little between storm periods. The highest tide during this study occurred in November 1981, after the equilibrium point had already begun shifting toward the two-bar configuration. It was, therefore, not the initiating factor in the profile rotation. This increase in the mean water level obviously contributed to the overall beach changes, however.

The only attribute of the stormy periods that is possibly associated with large changes in profile slope and bar/trough pattern is the duration of unidirectional longshore currents. In all but one storm event (Tropical Storm Emily), southbound longshore currents were documented for periods of eight to ten days.

Miller et al. (1983) have documented similar situations at the FRF. They noted that the pier can cause very pronounced effects on the FRF bathymetry. The shoreline updrift of the pier erodes, while it builds up downdrift of the pier during periods of unidirectional longshore transport.

Pre-existing morphology is an important factor in controlling the subsequent profile changes and supports the concept of sequential beach stage models proposed by Sonu and Van Beek (1971) and Wright et al. (1979). At the Duck site the magnitude of change toward the equilibrium bar/trough configuration is a function of the bar/trough configuration before the storm occurred. It was also found that the magnitude of the profile slope change during a storm is a function of the pre-storm profile slope.

A single shoreline crescentic wave is usually present at the Duck site with a wave length equal to the reach surveyed by the CRAB. Crescentic forms in this size class have been previously reported along the Outer Banks by Vincent (1973). The amplitude of profile elevations along the crescentic form is greatest seaward of 300 m from the FRF baseline. Because the crescentic form involves the profile rotation eigenfunction, it seems apparent that these crescentic forms are directly associated with onshore-offshore sediment exchanges. During the October and November storms sediment was transported offshore.

The offshore sediment exchanges of October and November occurred simultaneously across three zones. Sediment was moved from the beach to the nearshore where a bar was formed. Mid-profile sediments from the region of the summer bar were moved to the winter bar position. Sediments seaward of 800 m were moved farther seaward. The spacing

between these three zones is 250 m. The November changes in the subaerial, mid-profile, and deep water occurred at the same time even though the environmental variables were not significantly different from other storm events where no major morphologic changes were observed.

BIBLIOGRAPHY

Aubrey, D.G., 1979. Seasonal patterns of onshore/offshore sediment movement: Jour. Geophys. Res., v. 84, p. 6347-6354.

Aubrey. D.G., Inman, D.L., and Winant, C.D., 1980. The statistical prediction of beach changes in Southern California: Jour. Geophys. Res., v. 85, p. 3264-3276.

Birkemeier, W.A., DeWall, A.E., Gorbics, C.S., and Miller, H.C., 1981. A user's guide to CERC's Field Research Facility: Misc. Report No. 81-7, 118 p.

Bosserman, K., and Dolan, R., 1968. The frequency and magnitude of extratropical storms along the Outer Banks of North Carolina: Technical Report 68-4, National Park Service, 54 p.

Bowen, A.J., and Inman, D.L., 1971. Edge waves and crescentic bars: Jour. Geophys. Res., v. 76, p. 8662-8761.

Carter, T.G., Liu, P.L.-F., and Mei, C.C., 1973. Mass transport by waves and offshore bedforms: Jour. Waterways, Harbors and Coast. Eng., ASCE, WWR, p. 165-184.

Dalrymple. R.A., 1975. A mechanism for rip current generation on an open coast: Jour. Geophys. Res., v. 80, p. 3485-3487.

Dolan, R., 1966. Beach changes on the Outer Banks of North Carolina: Assoc. Am. Geographers Annals, v. 56, p. 699-711.

Dolan, R., and Hayden, B.P., 1979. Shoreline periodicities and edge waves: Jour. of Geol., v. 87, p. 175-185.

_____, 1981. Storms and shoreline configuration: Jour. of Sed. Petrol., v. 51, p. 737-744.

Dolan, R., Hayden, B.P., and Shabica, S.V., 1982. Beach morphology and inshore bathymetry of Horn Island, Mississippi: Jour. Geol., v. 90, p. 509-544.

Evans, O.F., 1940. The low and ball of the eastern shore of Lake Michigan: Jour. Geol., v. 48, p. 476-511.

Fox, W.T., and Davis, R.A., 1976. Weather patterns and coastal processes: In: R.A. Davis and R.L. Ethington (eds.), Beach and Nearshore Sedimentation Spec. Publication 24. Soc. Econ. Paleontologists and Mineralogists, p. 1-23.

Gilman, D.L., 1957. Empirical orthogonal functions applied to thirty-day forecasting: Unclassified Sci. Reports, Contract A-F 19(604)-1283. 120 p.

Goldsmith, V., Bowman, D., and Kiley, K., 1982. Sequential stage development of crescentic bars: Hahoterim Beach, Southeastern Mediterranean: Jour. of Sed. Petrol., v. 52, p. 233-249.

Guza, R.T., and Inman, D.L., 1975. Edge waves and beach cusps: Jour. Geophys. Res., v. 80, p. 2997-3012.

Hayden, B.P., 1981. Secular variation in Atlantic coast extra-tropical cyclones: Mon. Wea. Rev., v. 109, p. 159-167.

Hayden, B.P., Felder, W., Fisher, J., Resio, D., Vincent, L., and Dolan, R., 1975. Systematic variations in inshore bathymetry: ONR Technical Report 10. 64 p.

Kochel, R.C., Hayden, B.P., Dolan, R., Kahn, J.H., and May, P.F., 1983. Mid-Atlantic barrier coast classification: ONR Technical Report 27. 86 p.

Kochel, R.C., Hayden, B.P., Wayland, R.A., and Kahn, J.H., 1984. Spatial and temporal variations in mid-Atlantic nearshore bar morphology: ONR Technical Report 30, (in press).

Kutzbach, J., 1967. Empirical eigenvectors of sea-level pressure, surface temperature and precipitation complexes over North America: Jour. Appl. Meteor., v. 6, p. 791-802.

Lau, J., and Travis, B., 1973. Slowly varying Stokes waves and submarine longshore bars: Jour. Geophys. Res., v. 78, p. 4489-4497.

Lawrence, M.B., and Pelissier, J.M., 1982. North Atlantic tropical storm cyclones, 1981: Mar. Wea. Log, v. 26, p. 4-9.

_____, 1982. Atlantic hurricane season of 1981: Mon. Wea. Rev., v. 110. p. 852-866.

Lorenz, E., 1956. Empirical orthogonal functions and statistical weather prediction: Sci. Report 1, Dept. of Meteorology, MIT, 49 p.

Mariner's Weather Log, 1982. North Atlantic weather log: October, November, December: v. 26, p. 81-88.

Miller, H.C., and Leffler, M.W., 1981. Basic environmental data summary: November, 1981: CERC, FRF Publication, 28 p.

_____, 1982. Basic environmental data summary: August, 1982: CERC, FRF Publication, 28 p.

Miller, H.C., Birkemeier, W.A., and DeWall, A.E., 1983. Effects of CERC Research Pier on processes. Proceedings of Coastal Structures '83: New York: ASCE, p. 769-784.

Overland, J.E., and Preisendorfer, R.W., 1982. A significance test for principal components applied to a cyclone climatology: Mon. Wea. Rev., v. 110, p. 1-4.

Resio, D., Hayden, B.P., Dolan, R., and Vincent, L., 1974. Systematic variations in offshore bathymetry: ONR Technical Report 9, 39 p.

Shepard, F.P., 1950. Longshore bars and longshore troughs: U.S. Army Corps of Engineers, Beach Erosion Board Technical Memo., No. 15, 31 p.

Short, A.D., 1979, Three-dimensional beach stage model: Jour. of Geol., v. 87, p. 533-572.

Sonu, C.J., and Van Beek, J., 1971. Systematic beach changes on the Outer Banks, North Carolina: Jour. of Geol., v. 79, p. 416-425.

Vincent, L., 1973. Quantification of shoreline meandering: ONR Technical Report 7, 95 p.

Wright, L.D., Chappell, J., Thom, B.G., Bradshaw, M.P., and Cowell, P., 1979. Morphodyhamics of reflective and dissipative beach and inshore systems: Southeastern Australia: Marine. Geol., v. 32, p. 105-140.

Zeigler, J.M., Hayes, C.R., and Tuttle, S.D., 1959. Beach changes during storms on Outer Cape Cod, Massachusetts: Jour. of Geol., v. 67, p. 318-336.

REPORT DOCUMENTATION PAGE		READ INSTRUCTIONS BEFORE COMPLETING FORM
1. REPORT NUMBER Technical Report No. 29	2. GOVT ACCESSION NO.	3. RECIPIENT'S CATALOG NUMBER
4. TITLE (and Subtitle) Shorezone Profile Dynamics		5. TYPE OF REPORT & PERIOD COVERED Technical Report
		6. PERFORMING ORG. REPORT NUMBER
7. AUTHOR(s) Robert J. Wayland, Bruce P. Hayden		8. CONTRACT OR GRANT NUMBER(s) N00014-81-K-0033
9. PERFORMING ORGANIZATION NAME AND ADDRESS Department of Environmental Sciences University of Virginia Charlottesville, Virginia 22903		10. PROGRAM ELEMENT, PROJECT, TASK AREA & WORK UNIT NUMBERS NR389-170
11. CONTROLLING OFFICE NAME AND ADDRESS Office of Naval Research Coastal Sciences Program Arlington, Virginia 22217		12. REPORT DATE March 1984
		13. NUMBER OF PAGES 63
14. MONITORING AGENCY NAME & ADDRESS(if different from Controlling Office)		15. SECURITY CLASS. (of this report)
		15a. DECLASSIFICATION/DOWNGRADING SCHEDULE

16. DISTRIBUTION STATEMENT (of this Report)

Approved for public release, distribution unlimited

17. DISTRIBUTION STATEMENT (of the abstract entered in Block 20, if different from Report)

18. SUPPLEMENTARY NOTES

19. KEY WORDS (Continue on reverse side if necessary and identify by block number)

Principal Components Analysis, Beach Profile, Beach Changes, Storm Beach, Bars and Troughs

20. ABSTRACT (Continue on reverse side if necessary and identify by block number)

Principal components analysis was used to quantify subaerial and subaqueous summer to winter nearshore morphological change on the North Carolina coast near Duck. The first two eigenvectors explained 61.1% of the total variance. E1 (35.4% of the variance) is a profile rotation and E2 (25.7% of the variance) is a bar/trough function. Two major periods of change were found. High pressure systems in October and

DD ₁ FORM 73 1473   EDITION OF 1 NOV 65 IS OBSOLETE
S/N 0102-014-6601 |

SYSTEMATIC GEOGRAPHY LISTING

0001	1	OFFICE OF NAVAL RESEARCH	2 COPIES
0001	2	GEOGRAPHY PROGRAMS	
0001	3	CODE 462	
0001	4	ARLINGTON, VIRGINIA 22217	

0002	1	DEFENSE DOCUMENTATION CENTER	12 COPIES
0002	2	CAMERON STATION	
0002	3	ALEXANDRIA, VIRGINIA 22314	

0003	1	DIRECTOR, NAVAL RESEARCH LAB	6 COPIES
0003	2	ATTENTION TECHNICAL INFORMATION OFFICER	
0003	3	WASHINGTON, D. C. 20375	

0004	1	DIRECTOR
0004	2	OFFICE OF NAVAL RESEARCH BRANCH OFFICE
0004	3	1030 EAST GREEN STREET
0004	4	PASADENA, CALIFORNIA 91101

0005	1	DIRECTOR
0005	2	OFFICE OF NAVAL RESEARCH BRANCH OFFICE
0005	3	536 SOUTH CLARK STREET
0005	4	CHICAGO, ILLINOIS 60605

0006	1	DIRECTOR
0006	2	OFFICE OF NAVAL RESEARCH BRANCH OFFICE
0006	3	495 SUMMER STREET
0006	4	BOSTON, MASSACHUSETTS 02210

0007	1	COMMANDING OFFICER
0007	2	OFFICE OF NAVAL RESEARCH BRANCH OFFICE
0007	3	BOX 39
0007	4	FPO NEW YORK 09510

0008	1	CHIEF OF NAVAL RESEARCH
0008	2	ASST. FOR MARINE CORPS MATTERS
0008	3	CODE 100M
0008	4	OFFICE OF NAVAL RESEARCH
0008	5	ARLINGTON, VIRGINIA 22217

0009	1	OFFICE OF NAVAL RESEARCH
0009	2	CODE 480
0009	3	NATIONAL SPACE TECHNOLOGY LABORATORIES
0009	4	BAY ST. LOUIS, MISSISSIPPI 39520

0010	1	OFFICE OF NAVAL RESEARCH
0010	2	OPERATIONAL APPLICATIONS DIVISION
0010	3	CODE 200
0010	4	ARLINGTON, VIRGINIA 22217

SYSTEMATIC GEOGRAPHY LISTING

0011	1	OFFICE OF NAVAL RESEARCH
0011	2	SCIENTIFIC LIAISON OFFICER
0011	3	SCRIPPS INSTITUTION OF OCEANOGRAPHY
0011	4	LA JOLLA, CALIFORNIA 92093
0012	1	DIRECTOR, NAVAL RESEARCH LABORATORY
0012	2	ATTN LIBRARY, CODE 2628
0012	3	WASHINGTON, D. C. 20375
0013	1	ONR SCIENTIFIC LIAISON GROUP
0013	2	AMERICAN EMBASSY — ROOM A-407
0013	3	APO SAN FRANCISCO 96503
0101	1	COMMANDER
0101	2	NAVAL OCEANOGRAPHIC OFFICE LIBRARY
0101	3	XXXXXXXXXXXXXXXXXXXXX NAVOCEANO - NSTL STATION
0101	4	XXXXXXXXXXXXXXXXXXXXX BAY ST. LOUIS, MISSISSIPPI 39522
0102	1	NAVAL OCEANOGRAPHIC OFFICE
0102	2	XXXXXXXXXX NSTL STATION
0102	3	XXXXXXXXXXXXXXXXXXXXX BAY ST. LOUIS, MISSISSIPPI 39522
0103	1	CHIEF OF NAVAL OPERATIONS
0103	2	OP 987P1
0103	3	DEPARTMENT OF THE NAVY
0103	4	WASHINGTON, D. C. 20350
0104	1	OCEANOGRAPHER OF THE NAVY
0104	2	HOFFMAN II BUILDING
0104	3	200 STOVALL STREET
0104	4	ALEXANDRIA, VIRGINIA 22322
0105	1	NAVAL ACADEMY LIBRARY
0105	2	U. S. NAVAL ACADEMY
0105	3	ANNAPOLIS, MARYLAND 21402
0106	1	COMMANDING OFFICER
0106	2	NAVAL COASTAL SYSTEMS LABORATORY
0106	3	PANAMA CITY, FLORIDA 32401
0107	1	LIBRARIAN
0107	2	NAVAL INTELLIGENCE
0107	3	SUPPORT CENTER
0107	4	4301 SUITLAND ROAD
0107	5	WASHINGTON, D. C. 20390

OCT. 26, 1977   JOB 460-101

SYSTEMATIC GEOGRAPHY LISTING

0112	1	OFFICER IN CHARGE
0112	2	ENVIRONMENTAL RESEARCH PRDCTN FCLTY
0112	3	NAVAL POSTGRADUATE SCHOOL
0112	4	MONTEREY, CALIFORNIA 93940
0201	1	COMMANDING GENERAL
0201	2	MARINE CORPS DEVELOPMENT AND
0201	3	EDUCATIONAL COMMAND
0201	4	QUANTICO, VIRGINIA 22134
0202	1	DR. A. L. SLAFKOSKY
0202	2	SCIENTIFIC ADVISOR
0202	3	COMMANDANT OF THE MARINE CORPS
0202	4	CODE MC-RD-1
0202	5	WASHINGTON, D. C. 20380
1001	1	DEFENSE INTELLIGENCE AGENCY
1001	2	CENTRAL REFERENCE DIVISION
1001	3	CODE RDS-3
1001	4	WASHINGTON, D. C. 20301
1002	1	DIRECTOR
1002	2	DEFENSE MAPPING TOPOGRAPHIC CENTER
1002	3	ATTN= CODE 50200
1002	4	WASHINGTON, D. C. 20315
1003	1	COMMANDING OFFICER
1003	2	U.S. ARMY ENGINEERING
1003	3	TOPOGRAPHIC LABORATORY
1003	4	ATTN= ETL-ST
1003	5	FORT BELVOIR, VIRGINIA 22060
1005	1	CHIEF, WAVE DYNAMICS DIVISION
1005	2	USAE-WES
1005	3	P. O. BOX 631
1005	4	VICKSBURG, MISSISSIPPI 39180
2003	1	NATIONAL OCEANOGRAPHIC DATA
2003	2	CENTER ID764
2003	3	ENVIRONMENTAL DATA SERVICES
2003	4	NOAA
2003	5	WASHINGTON, D. C. 20235
2005	1	CENTRAL INTELLIGENCE AGENCY
2005	2	ATTENTION OCR/DD-PUBLICATIONS
2005	3	WASHINGTON, D. C. 20505

SYSTEMATIC GEOGRAPHY LISTING

2007	1	DR. MARK M. MACOMBER
2007	2	ADVANCED TECHNOLOGY DIVISION
2007	3	DEFENSE MAPPING AGENCY (DELETED)
2007	4	NAVAL OBSERVATORY
2007	5	WASHINGTON, D. C. 20390

5001	1	MINISTERIALDIREKTOR DR. F. WEVER
5001	2	RUE/FO
5001	3	BUNDESMINISTERIUM DER VERTEIDIGUNG
5001	4	HARDTHOEHE
5001	5	D-5300 BONN, WEST GERMANY

5002	1	OBERREGIERUNGSRAT DR. ULLRICH
5002	2	RUE/FO
5002	3	BUNDESMINISTERIUM DER VERTEIDIGUNG
5002	4	HARDTHOEHE
5002	5	D-5300 BONN, WEST GERMANY

5003	1	MR. TAGE STRARUP
5003	2	DEFENCE RESEARCH ESTABLISHMENT
5003	3	OSTERBROGADES KASERNE
5003	4	DK-2100 KOBENHAVN O, DENMARK

5302	1	IR. M. W. VAN BATENBERG
5302	2	PHYSISCH LABORATORIUM TNO
5302	3	OUDE WAALSDORPER WEG 63, DEN HAAG
5302	4	NETHERLANDS

8002	1	COASTAL STUDIES INSTITUTE
8002	2	LOUISIANA STATE UNIVERSITY
8002	3	BATON ROUGE, LOUISIANA 70803

8003	1	DR. CHOULE J. SONU
8003	2	TEKMARINE, INC.
8003	3	37 AUBURN AVENUE
8003	4	SIERRA MADRE, CA 91024

9001	1	DR. LESTER A. GERHARDT
9001	2	RENNSSELAER POLYTECHNIC INSTITUTE
9001	3	TROY, NEW YORK 12181

9002	1	MR. FRED THOMSON
9002	2	ENVIRONMENTAL RESEARCH INSTITUTE
9002	3	P.O. BOX 618
9002	4	ANN ARBOR, MICHIGAN 48107

SYSTEMATIC GEOGRAPHY LISTING

```
9004  1  DR. THOMAS K. PEUCKER
9004  2  SIMON FRASER UNIVERSITY
9004  3  DEPARTMENT OF GEOGRAPHY
9004  4  BURNABY 2, B. C., CANADA

9005  1  DR. ROBERT DOLAN
9005  2  DEPARTMENT OF ENVIRONMENTAL SCIENCES
9005  3  UNIVERSITY OF VIRGINIA
9005  4  CHARLOTTESVILLE, VIRGINIA 22903
```

END

FILMED

5-84

DTIC